Universidade do Porto

FEUP Faculdade de Engenharia

**Catarina Cardoso Coelho**

# Heparinized nanohydroxyapatite/collagen granules for controlled release of vancomycin

**Porto**

**July 2013**

**Catarina Cardoso Coelho**

# Heparinized nanohydroxyapatite/collagen granules for controlled release of vancomycin

Work presented to Faculdade de Engenharia da Universidade do Porto as part of the requirements for the Degree of Master in Biomedical Engineering under the supervision of Professor Fernando Jorge Monteiro from Faculdade de Engenharia da Universidade do Porto (FEUP) and Professor Susana Sousa from Instituto Superior de Engenharia/Instituto Politécnico do Porto (ISEP/IPP).

# Acknowledgments

I would like to express my gratitude to all the people that helped me during the development of this work and contributed to make it possible.

First, I will start to express my gratitude to my supervisors, Prof. Dr. Fernando Jorge Monteiro and Prof. Dr. Susana Sousa for the great opportunities that they gave me and all the support, guidance, patience and friendship.

I also want to acknowledge all members of Biocomposites group for the help and friendship during this journey. Some of you started as simple colleagues and ended as amazing friends. Very special thanks to Susana Neves for everything she did for me. I do not have enough words to express my gratitude as you helped me in so many things. I must highlight your help with cell culture assays as your contribution was essential to my success. I acknowledge Marta Laranjeira for guiding me during the first steps of my work and helping me with my difficulties related with granules. In addition, I want to thank Ângela Carvalho for many subjects that she helped me, particularly with bacterial adhesion assays. Moreover, I acknowledge Joana Barros for assistance and availability to help me with bioactivity assays. I also want to thank Liliana Grenho for her help with microbiology subjects. I want to thank Eugénia Queirós and Mariline Pinto for all their assistance during my work and for supporting me so many times. Without all these people, an important part of my work would not be possible. The Biocomposites group is a great example of how it is important to collaborate and work as a team. It was a pleasure to work with you all. Thank you so much.

From INEB, I want to acknowledge Ricardo Vidal for all the help and great ideas to improve my work. I also show my gratitude to Maria Lázaro for the assistance during confocal microscopy studies. Joana Antunes is greatly acknowledged for all the useful suggestions to enrich my work. And I also want to thank my friends Vanessa Graça and Catarina Seabra, not only for the all the support, but also for the funny moments that made this journey even more remarkable.

From FEUP, I express my gratitude to Dr. Aurora Futuro for the sieves she kindly lent me and Sr. Ramiro for the all assistance during my work.

From UFP, I want to thank Prof. Maria Pia Ferraz and the technician Ricardo Silva for all their assistance during the work I developed at CEBIMED laboratory.

From CEMUP, I acknowledge Daniela Silva and Rui Rocha for all the help related with SEM analysis.

From 3B's Research Group, I want to acknowledge Dr. Vitor Correlo for the help with Micro-CT analysis and its results. During this visit to 3B's, I also want to thank my old friend Ana Rita Santos and her friends for their friendship and hospitality.

I greatly acknowledge Fluidinova S.A. for the provision of nanoHA powder and the project NanoForBone (Ref NORTE-01-0202-FEDER-005372) for funding.

Besides, I want to acknowledge my friends for all the support they gave me and for being always interested in my work. A special thanks to Ricardo Borges for his company during some working days.

I also want to express my gratitude to Tiago Peres, for the good advices he gave me during this journey and for all his support during the past years, always encouraging me and believing in my decisions.

Above all, I want to acknowledge my family for the support during this journey and for making my life easier so that I could dedicate myself to this project. I thank my father and Luísa for being so understanding and supportive. Carlos is also greatly acknowledged for being so interested in my work and for always wishing my success. Moreover, I thank my mother and my aunt Fátima, for being always worried about my well-being and for encouraging me every day. This work is dedicated to you both.

# Abstract

Osteomyelitis is a bone infection that can be caused by a variety of microorganisms, being *Staphylococcus aureus* (*S. aureus*) the most common pathogen involved and resulting in tissue necrosis. Vancomycin is a glycopeptide antibiotic known to be effective against *S. aureus* and currently used in cases of osteomyelitis. An ideal strategy for the treatment of this infection would combine the eradication of the pathogen and simultaneously the induction of bone tissue regeneration.

Nanohydroxyapatite (nanoHA) and collagen composites had already been used as materials for bone applications due to the similarity with native tissue and their capacity to be osteoconductive and bioactive, enhancing bone formation. Moreover, these materials are able to be used as drug vehicles, although they do not always present an adequate drug releasing profile. Heparin is a glycosaminoglycan known to interact with several relevant biomolecules, such as proteins and growth factors. Therefore, coating a biomaterial with heparin may result in a development of a localized drug delivery system, capable to perform a sustainable release of those important biomolecules.

The aim of this work was to develop heparinized nanoHA/collagen granules able to release vancomycin to be used in treatment of osteomyelitis and to induce the formation of new bone. Characterization studies with Scanning Electron Microscopy (SEM) and X-ray Micro-Computed Tomography (Micro-CT) shown that the produced biocomposite has high surface area and porosity, particularly macro, micro and nanoporosity. These granules were able to release higher amounts of vancomycin in a controlled manner, when compared with non-heparinized granules. Moreover, vancomycin released levels were capable to inhibit *S. aureus* growth considered also non-toxic. The heparinized granules also presented higher *S. aureus* adhesion which may improve the treatment effectiveness. Finally, a preliminary osteoblast culture indicated that vancomycin affected the metabolic activity of these cells in the first week of culture, when antibiotic concentrations were higher. However, after 14 days of culture, when vancomycin release almost ceased, the remaining viable cells were able to recover and proliferate as demonstrated by metabolic activity, SEM and Confocal Laser Scanning Microscopy (CLSM). A novel material of nanoHA/collagen capable of being grafted with heparin was successfully produced allowing a sustained release of vancomycin. These granules may be considered a promising biocomposite for the treatment of osteomyelitis since they were able to inhibit *S. aureus* growth and are expected to induce bone tissue regeneration.

**Keywords:** osteomyelitis, *S. aureus*, vancomycin, nanohydroxyapatite, collagen, heparin.

# Resumo

A osteomielite é uma infeção no osso que pode ser causada por uma diversidade de microorganismos, sendo a bactéria *Staphylococcus aureus* (*S. aureus*) o patogénio mais frequentemente envolvido, levando à necrose do osso. A vancomicina é um antibiótico glicopeptídico conhecido por ser eficaz contra a *S. aureus* e usado atualmente em casos de osteomielite. Uma estratégia ideal para o tratamento desta infeção combinaria a erradicação do patogénio e, simultaneamente, a indução da regeneração do tecido ósseo.

Compósitos de nanohidroxiapatite (nanoHA) e colagénio foram anteriormente usados como materiais para aplicação no osso pela sua semelhança com o tecido nativo e capacidade de osteocondução e bioatividade. Estes materiais podem ainda ser usados como veículos transportadores para fármacos, embora nem sempre possuam o perfil de libertação adequado. A heparina é um glicosaminoglicano conhecido por interagir com várias moléculas relevantes, como proteínas e fatores de crescimento. Imobilizar heparina num biomaterial pode resultar no desenvolvimento de um sistema controlado de libertação de proteínas e fatores de crescimento.

O objetivo deste trabalho foi o desenvolvimento de grânulos heparinizados de nanoHA/colagénio capazes de libertar localmente e de uma forma sustentada vancomicina para o tratamento da osteomielite, induzindo a formação de novo tecido ósseo. Estudos de caraterização com Microscopia Eletrónica de Varrimento (SEM) e Microtomografia Computadorizada de raios-X (Micro-CT) demonstraram que estes grânulos têm elevada área superficial e porosidade, em particular macro, micro e nanoporosidade. Estes grânulos foram capazes de libertar níveis mais elevados de vancomicina e de uma forma controlada, quando comparados com grânulos não-heparinizados. Além disso, a vancomicina foi libertada em concentrações capazes de inibir o crescimento de *S. aureus* e em níveis considerados não-tóxicos. Os grânulos heparinizados possuem uma maior adesão de *S. aureus*, o que poderá melhorar a eficácia do tratamento. Por fim, uma cultura preliminar de osteoblastos demonstrou que a vancomicina afeta a atividade metabólica destas células na primeira semana de cultura, a fase em que as concentrações de antibiótico foram mais elevadas. Porém, após 14 dias de cultura, quando a libertação de vancomicina quase terminou, as células que permaneceram viáveis foram capazes de recuperar e proliferar, como verificado através da atividade metabólica, SEM e Microscopia Confocal de Varrimento a Laser (CLSM).

Desta forma, um novo material de nanoHA/colagénio capaz de ser revestido com heparina e libertar vancomicina de uma forma controlada foi produzido com sucesso. Estes grânulos

podem ser considerados um biocompósito promissor para o tratamento da osteomielite visto serem capazes de inibir o crescimento de *S. aureus* e induzir a regeneração do tecido ósseo.

**Palavras-chave:** osteomielite, *S. aureus*, vancomicina, nanohidroxiapatite, colagénio, heparina

# Contents

# List of figures

# List of tables

# List of abbreviations

2D - two dimensional

3D - three dimensional

ALP - alkaline phosphatase

ATR-FTIR - Attenuated Total Reflectance-Fourier Transformed Infrared Spectroscopy

BMP-2 - bone morphogenetic protein-2

BSA - bovine serum albumin

cAMP - cyclic adenosine monophosphate

CFU - colony-forming unit

CLSM - Confocal Laser Scanning Microscopy

DA - dispersive agent

DDS - drug delivery system

ECM - extracellular matrix

EDC - *N*-(3-dimethylaminopropyl)-*N*'-ethylcarbodiimide

EDS - Energy-dispersive X-ray Spectroscopy

FBS - fetal bovine serum

FTIR - Fourier Transformed Infrared Spectroscopy

HA - hydroxyapatite

Hep - heparinized

MES - 2-mofpholinoethane sulfonic acid

MIC - minimum inhibitory concentration

Micro-CT - X-ray Micro-Computed Tomography

MRSA - methicillin-resistant *S. aureus*

MTC - minimum toxic concentration

NAG - *N*-acetylglucosamine

NAM - *N*-acetylmuramic acid

NanoHA - nanohydroxyapatite

NHS - *N*-hydroxysuccinimide

PBPs - penicillin-binding proteins

PBS - phosphate buffer saline

PFA - paraformaldehyde

pI - isoelectric point

PU - polyurethane

RFU - relative fluorescence units

RT - room temperature

SEM - Scanning Electron Microscopy

TCPS - tissue culture polystyrene

TSST-1 - toxic shock syndrome toxin 1

VRSA - vancomycin-resistant *S.aureus*

α-MEM - alpha minimum essential medium

# Chapter 1: Introduction

## 1.1. Bone tissue

### 1.1.1. Overview

Bone tissue is the one of the hardest tissues of the human body, together with enamel and dentin, but still one of the most dynamic ones (1). The main function of bone is to give structural support and locomotion capability to the body. Bones give protection to some vital organs, such as brain, heart and lungs. Moreover, this tissue is highly vascularized and gives support to hematopoiesis in the bone marrow. In addition, bone is the attachment for muscles, ligaments and tendons, supporting muscle contraction. This tissue has the unique ability to heal and remodel without leaving a scar, thus being capable to repair factures or other defects (2, 3). However, if bone tissue presents a defect above a critical size, it becomes impossible to self-heal. These situations represent a major problem in regenerative medicine (4). Bone is also a mineral pool, in particular for the regulation of calcium. Considering the important roles of bone, it is easily concluded that alterations in its structure related to injury or disease can change significantly the body's equilibrium and the quality of life of patients (2).

### 1.1.2. Bone matrix composition

Bone is a composite material as its matrix is constituted by an inorganic and an organic portion. The inorganic portion is the calcified region of bone (approximately 65 % of the dry weight) and it is composed mainly by non-stoichiometric calcium phosphate mineral apatite, mainly of hydroxyapatite (HA) crystals ($Ca_{10}(PO_4)_6(OH)_2$), containing low percentages of bicarbonate, magnesium, citrate and sodium among other ions. The organic portion (approximately 35 % of the dry weight) is constituted essentially by type I collagen (5). The collagen is presented as fibrils (approximately 50-70 nm diameter) mostly crosslinked (1), where the HA crystals (10-50 nm in length) are stuck and can grow (6). The sizes and orientation of the HA crystals are determined specifically by the collagen template, as the crystals are disposed along the collagen fibers (Figure 1). This structural relationship between collagen fibrils and HA crystals is essential for bone's resilience and strength (6). If all the mineral component is removed from bone, this tissue is able to retain its original shape but becomes extremely flexible being easily twisted like a piece of rubber. However, if the organic component is removed, the mineral part is able to maintain the original shape but it

turns out to be very brittle and easily fractured (1). The surface ions of HA crystals also interact with water, attracting it and forming a hydration shell. The latter allows ion exchange with the extracellular fluid (1).

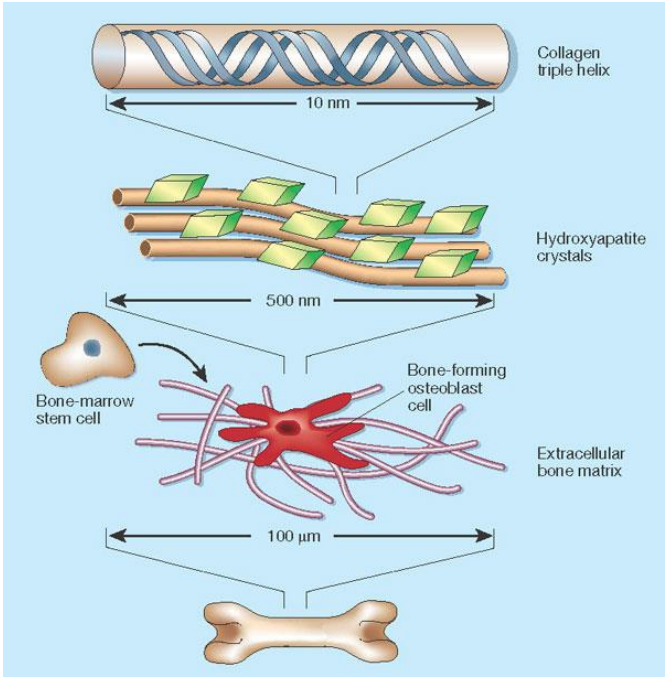


**Figure 1:** The many scales of organization in natural bone (6).

The organic portion has also a ground substance containing chondroitin sulfate and keratan sulfate. Besides collagen, there are also other matrix proteins such as osteocalcin, osteopontin and bone sialoprotein. Osteocalcin and osteopontin are glycoproteins that bind to hydroxyapatite and integrins in osteoblasts and osteoclasts (5). The synthesis of these two proteins is stimulated by Vitamin D (1). Bone sialoprotein is also capable of binding to integrins of osteoblasts and osteocytes. Therefore, this protein is associated with bone cells adhesion to the bone matrix (5).

### 1.1.3. Structure

Cross-sections of bone demonstrate the presence of two types of bones: compact (cortical or dense) bone and cancellous (trabecular or spongy) bone (Figure 2) (5). Compact bone is present in many small and shallow bones. In longer bones, it is located at the periphery, is denser, does not contain marrow and its blood vessels are microscopically small (1, 7). In opposition, cancellous bone is present in longer bones. This type of bone incases the bone marrow and it contains a large number of small blood vessels. It comprises a network of hard interconnected trabeculae and spicules that are extended from the internal surface of the compact bone into the marrow cavity. Concerning the

bone marrow, there are two different types, the yellow bone marrow, composed essentially of fat, and the red bone marrow, where the blood cells are formed. Cancellous bone possesses irregular arrangements of lamellae that contain osteocytes accommodated in their lacunae and coated by a single layer of osteoblasts (1, 5, 7).

The majority of compact bone is composed by osteons (or Havers systems) that are not present on cancellous bone (Figure 2) (1). These structures are considered the primary histological unit of bone and each system is formed by cylinders of lamellae, concentrically arranged around the haversian canal. The latter is considered the lumen of the osteon and it has fluid filling it and a blood vessel that supplies nourishment to the bone cells, and is lined by a layer of osteoprogenitor cells and osteoblasts (1, 7). In addition, each haversian canal accommodates a neurovascular bundle and its related connective tissue. Adjacent osteons can connect with each other by vascular spaces called Volkmann's canals (Figure 2). These canals connect two adjacent haversian canals and are oriented obliquely or perpendicularly to them. Each osteon is limited by thin cementing line of calcified matrix and slight amount of collagen fibers (1).

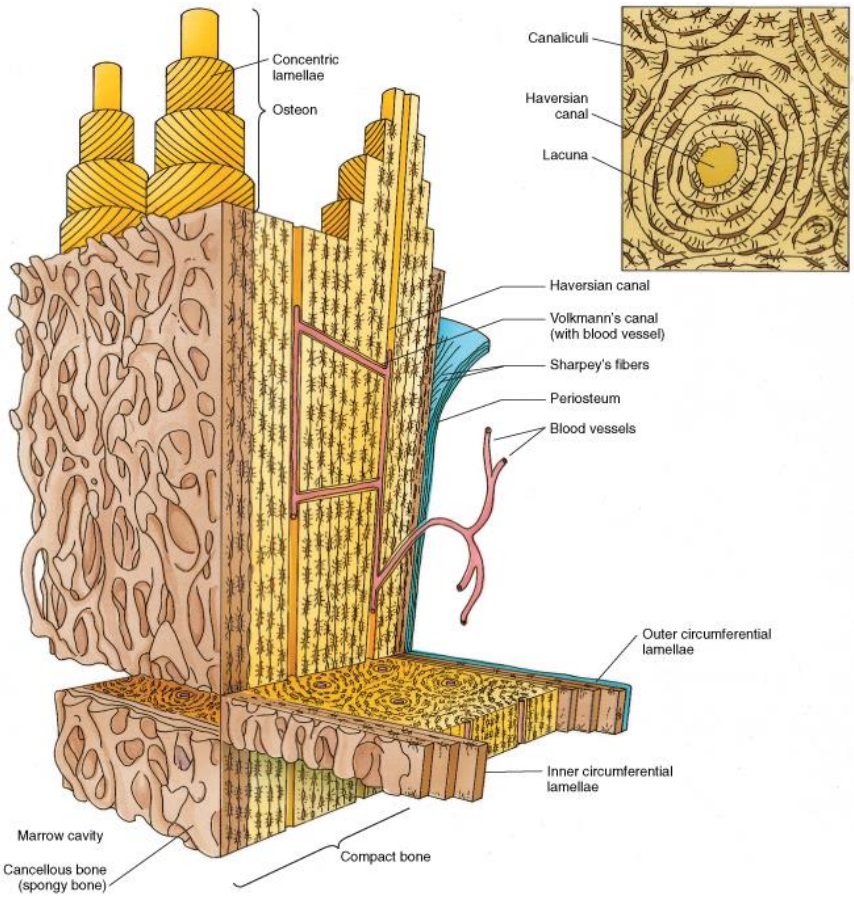


**Figure 2:** Diagram of bone illustrating compact bone, osteons, lamellae, Volkmann's canals, haversian canals, lacunae, canaliculi and cancellous bone (1).

Almost all bones are covered on their external surfaces by a layer of non-calcified connective tissue named as periosteum (except at muscle attachments and synovial articulations). The periosteum is constituted by an outer layer of dense fibrous collagen and an inner layer composed by osteoprogenitor cells. This dense connective tissue distributes blood vessels to bone and it is attached to the bone surface by Sharpey fibers (collagen type I) (1, 5). Coating the marrow cavities is a thin layer of connective tissue called endosteum that supplies osteoprogenitor cell and osteoblasts for bone growth and repair (5).

### 1.1.4. Bone cells

Bone tissue has four different types of cells: osteoprogenitor cells, osteoblasts, osteoclasts and osteocytes. Osteoprogenitor cells are derived from the embryonic mesenchyme, retained their capacity to undergo mitosis and are able to differentiate into osteoblasts (1, 5). Osteoblasts can have a cuboidal to columnar shape and they are situated at the bone surface forming a sheet-like arrangement (1). These cells synthesize the organic proteins of the matrix, such as collagen type I, glycoproteins and proteoglycans. Besides, they secrete osteocalcin and osteonectin for bone mineralization, osteopontin for the formation of the sealing zone between osteoclasts and the subosteoclastic compartment and bone sialoprotein that participates in binding of the osteoblasts to the extracellular matrix (ECM) (5). Alkaline phosphatase (ALP) enzyme is abundant in osteoblast cell membranes. These cells secrete high levels of ALP during active bone formation, increasing the levels of this enzyme in the blood. Therefore, bone formation can be measured by monitoring the levels of ALP in blood (1). While osteoblasts exocyte their secretion products during bone remodeling, these cells become entrapped in lacunae and are called osteocytes (1, 5). The latter seem to be inactive cells, but they secrete substances required for bone maintenance. These cells are involved in mechanotransduction, as they respond to stimuli on bone by producing cyclic adenosine monophosphate (cAMP), insulin-like growth factor and osteocalcin. These molecules improve the recruitment of pre-osteoblasts, in order to assist the bone remodeling (1). Osteoclasts are multinucleated cells originating from granulocyte-macrophage progenitors from bone marrow and they are responsible for bone resorption. They secret acid that decalcifies the surface layer of bones. Besides, these cells also secrete proteolytic enzymes such as collagenase that degrade bone organic portion. The organic and inorganic residues of the bone matrix are reabsorbed by osteoclasts and released into the capillaries (5).

## 1.1.5. Bone remodeling

The term “remodeling” refers to the continually undergoing processes of growth, reinforcement and resorption of living bone. The processes during remodeling allow living bone to adapt its histological structure to changes in long term loading (7). The bone remodeling is a cycle of highly regulated events that involves the interactions between two cell lineages, the mesenchymal osteoblastic lineage and the hematopoietic osteoclastic lineage (Figure 3). The primary stage of bone remodeling consists in the interaction between the osteoblast and osteoclast precursor cells, leading to the differentiation, migration and fusion of the multinucleated osteoclasts (8). Bone resorption is initiated with osteoclasts attachment to the mineralized bone surface and secretion of hydrogen ions and lysosomal enzymes (8). Inside the osteoclasts, the carbonic anhydrase enzyme produces carbonic acid from carbon dioxide and water. Then, the carbonic acid dissociates into hydrogen and bicarbonate ions. The hydrogen ions are released to the bone matrix decreasing the pH and causing the dissolution of HA crystals. The lysosomal enzymes are secreted to degrade the organic components of the matrix. The consequent degradation products are endocytosed by osteoclasts, once again degraded into amino acids, monosaccharides and disaccharides and released into capillaries (1).

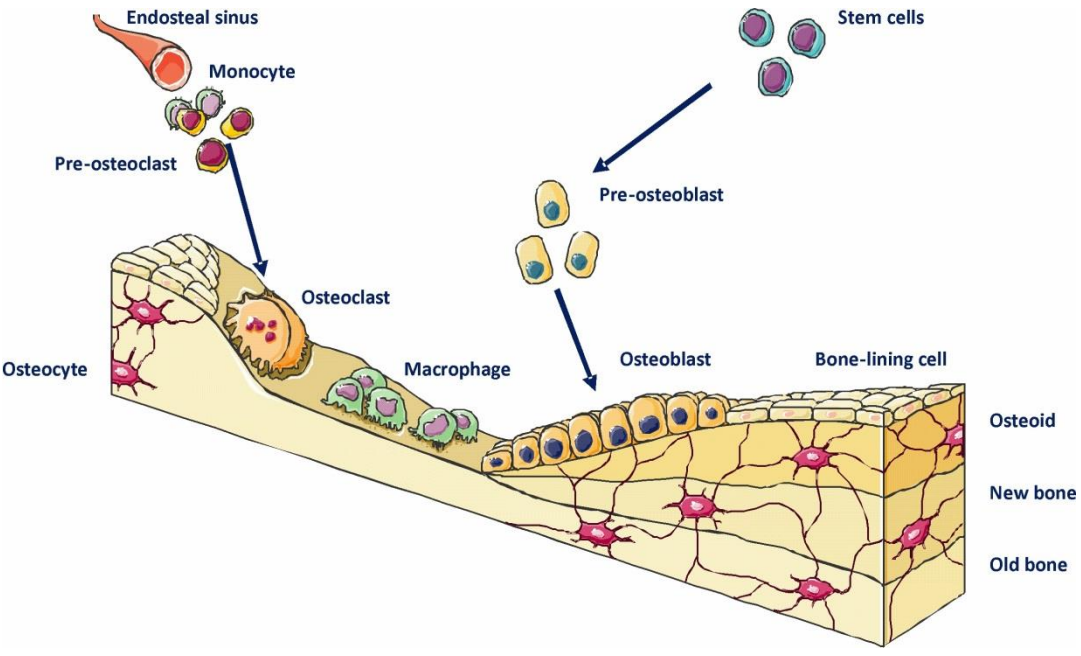


**Figure 3:** Bone remodeling osteoblasts and osteoclasts differentiation (9).

The resorption of the bone haversian systems creates absorption cavity as the osteocytes die. The increasing osteoclastic activity increases the diameter and length of the cavities. These are then invaded by blood vessels and the bone resorption ceases. Then, the cavities are completely filled by

consecutive layers of osteoblasts that start to deposit a mineralized matrix around the blood vessels, creating new haversian systems. Remodeling not only happens in primary bone but it also continues through life. The process of bone replacement after bone resorption is known as coupling (1, 8).

## 1.2. Osteomyelitis

### 1.2.1. Classification

Osteomyelitis is an infection of bone caused by microorganisms. This infection can be restricted to a single part of the bone or it can affect several regions (periosteum, cortex, marrow and the surrounding soft tissues). The evolution of the infection can cause bone necrosis (10). Traditionally, osteomyelitis has been characterized according to the time of occurrence of infection or injury as acute, sub-acute or chronic (11). The development of acute osteomyelitis occurs one or two weeks after disease onset, sub-acute osteomyelitis appears after one to few months and chronic osteomyelitis appears after several months. Osteomyelitis is a complex disease state and is difficult to classify. Many classification systems were made not only taking into account the general categories of acute, sub-acute and chronic (11). In a practical sense, it is possible to distinguish between three different types of osteomyelitis. Hematogenous osteomyelitis is characterized by the seeding of the bacteria from bloodstream and corresponds to 20 % of the osteomyelitis cases (12). Osteomyelitis can also emerge due to vascular insufficiency. This type of osteomyelitis occurs mainly in people with diabetes and follows a foot infection that spreads to bone. Finally, osteomyelitis can appear due to a bacterial spread from a contiguous contaminated source after trauma, bone surgery or joint replacement. In these situations, osteomyelitis can appear in any age and any bone (10).

### 1.2.2. Etiology

The microorganisms found in patients with osteomyelitis are often related with the age (Table 1) or the clinical scenario of the patient (11). *Staphylococcus aureus* (*S. aureus*) is the most frequently involved pathogen in this infection (10, 11, 13). This bacterium is involved in most cases of acute hematogenous osteomyelitis in children and adults. In newborns, the group B streptococcus is the main pathogen involved. In adults, *S. aureus* is the main pathogen involved in bone and prosthetic joint infections (13). Resistant strains such as methicillin-resistant *S. aureus* (MRSA) have been emerged and isolated from patients with osteomyelitis (13). Besides *S. aureus*, other microorganisms such as *Staphylococcus epidermidis*, *Pseudomonas aeruginosa*, *Escherichia coli* and *Serratia mascescens* are isolated from patients with chronic osteomyelitis (11). In addition, infections caused by fungal and mycobacterial have been identified in patients with osteomyelitis. However, these cases are rare and are normally found in patients with impaired immune function (13).

**Table 1:** Organisms frequently isolated from osteomyelitis cases based on patient age. Adapted from (11).

| Organisms Frequently Isolated in Osteomyelitis Based on Patient Age | | |
|---|---|---|
| **Infants (<1 year)** | **Children (1 to 16 years)** | **Adults (>16 years)** |
| Group B streptococci | *Staphylococcus aureus* | *Staphylococcus epidermidis* |
| *Staphylococcus aureus* | *Streptococcus pyogenes* | *Staphylococcus aureus* |
| *Escherichia coli* | *Haemophilus influenzae* | *Pseudomonas aeruginosa* |
| | | *Serratia marcescens* |
| | | *Escherichia coli* |

## 1.2.3. *Staphylococcus aureus*

As above mentioned, osteomyelitis can be caused by a variety of pathogenic microorganisms, but *S. aureus* is the most frequently involved (10). The infections caused by this microorganism are often associated with recent surgery, hospitalization, dialysis, catheters and percutaneous medical devices (14). *S. aureus* is a gram-positive coccus bacterium with a size of 0.5-1.5 μm (15) and it is the main cause of infections acquired in community or in hospitals (16). These gram-positive bacteria appear as grape-like clusters (Figure 4) and they have a typical cell wall consisted of a single 20-80 nm thick homogeneous layer of peptidoglycan situated outside the plasma membrane (Figure 5A) (17). The peptidoglycan from gram-positive cell walls is thicker, when compared to gram-negative bacteria (2-7 nm). This characteristic provides gram-positive bacteria a greater resistance to some environmental conditions such as osmotic pressure (17).

Peptidoglycan is a meshlike polymer composed by many similar subunits. This polymer is composed by two sugar derivatives, *N*-acetylmuramic acid (NAM) and *N*-acetylglucosamine (NAG), and many different amino acids. Three of these animo acids (D-glutamic acid, D-alanine and *meso*-diaminopimelic acid) are not present in proteins. The presence of D-amino acids in the peptidoglycan provides protection against degradation by peptidases, which are able to recognize only L-amino acids (17).

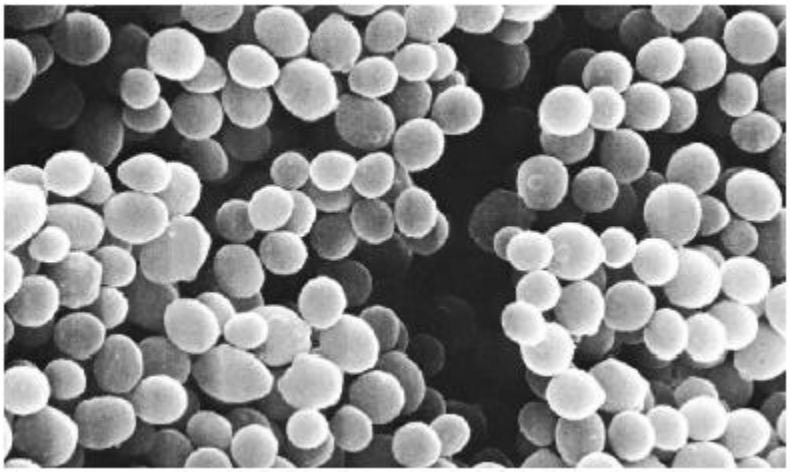

**Figure 4:** Scanning Electron Microscopy (SEM) depicted numerous clumps of *S. aureus*. 32000x magnification (17).

The backbone of the polymer is composed by the two sugars mentioned above. A chain consisting of four alternating D- and L- amino acids is linked to the carboxyl group of NAM. To obtain a strong, meshlike polymer, the peptidoglycan subunits are joined by cross-links between them. In the case of *S. aureus*, the peptidoglycan cross-link is made between the carboxyl group of D-alanine and the L-lysine with a peptide interbridge (Figure 5B). This type of crosslinking results in a great peptidoglycan sac, with a dense and interconnected network (17). *S. aureus* expresses bacterial adhesins at the surface that improve its attachment to the host ECM components, for instance fibrinogen, fibronectin, collagen, laminin, bone sialoprotein, vitronectin or elastin (Figure 6) (10, 18). The interactions between the bacteria and the host ECM proteins allow the early colonization of host tissues, biomaterials or both.

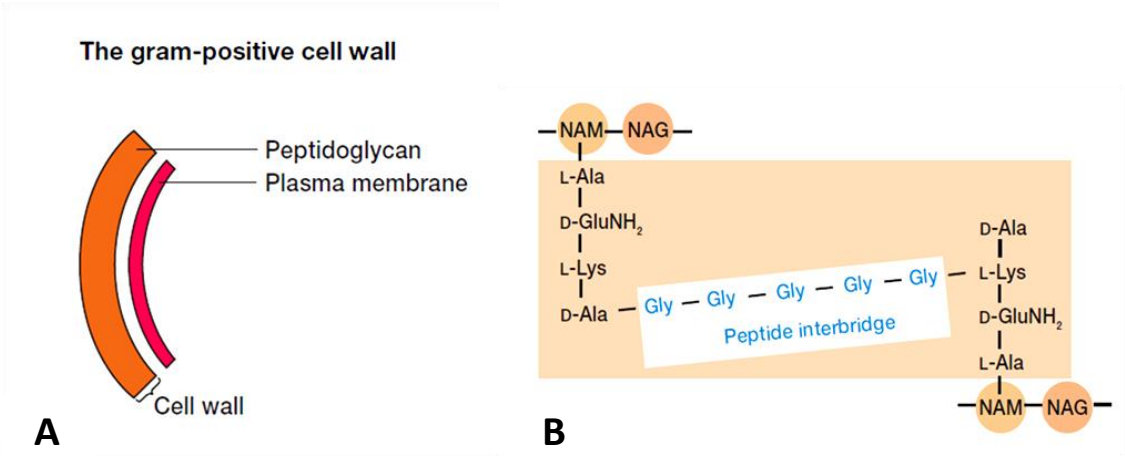


**Figure 5:** Characteristic gram-positive cell wall and *S. aureus* peptidoglycan. (A) The gram-positive cell wall. (B) *S. aureus* peptidoglycan. NAM: *N*-acetylmuramic acid. NAG: *N*-acetylglucosamine. Gly: Glycine. Adapted from (17).

Every year, around one million prosthetic devices for total hip replacement are implanted worldwide. These devices are susceptible to infections and more than 50 % of these infections are related with *S. aureus* (19). The latter can enter the cell by endocytosis, promoting its own invasion through endothelial or epithelial cells. Once inside the cell, this bacterium can acquire a modified metabolic state that improves its survival and persistence. Besides, *S. aureus* can express factors that promote their escape from the host immune system, such as protein A, some toxins and capsular polysaccharides (Figure 6). Therefore, this bacterium possesses a variety of mechanisms that allow its prevalence inside the host organism, which makes its eradication a hard task (10).

Another characteristic that makes *S. aureus* a difficult microorganism to treat is its ability to form a biofilm. A biofilm is defined as a "microbially derived sessile community, which is characterized by cells attached to a substrate, embedded in a polymeric ECM and having an altered phenotype with regard to growth, gene expression and protein production" (12).

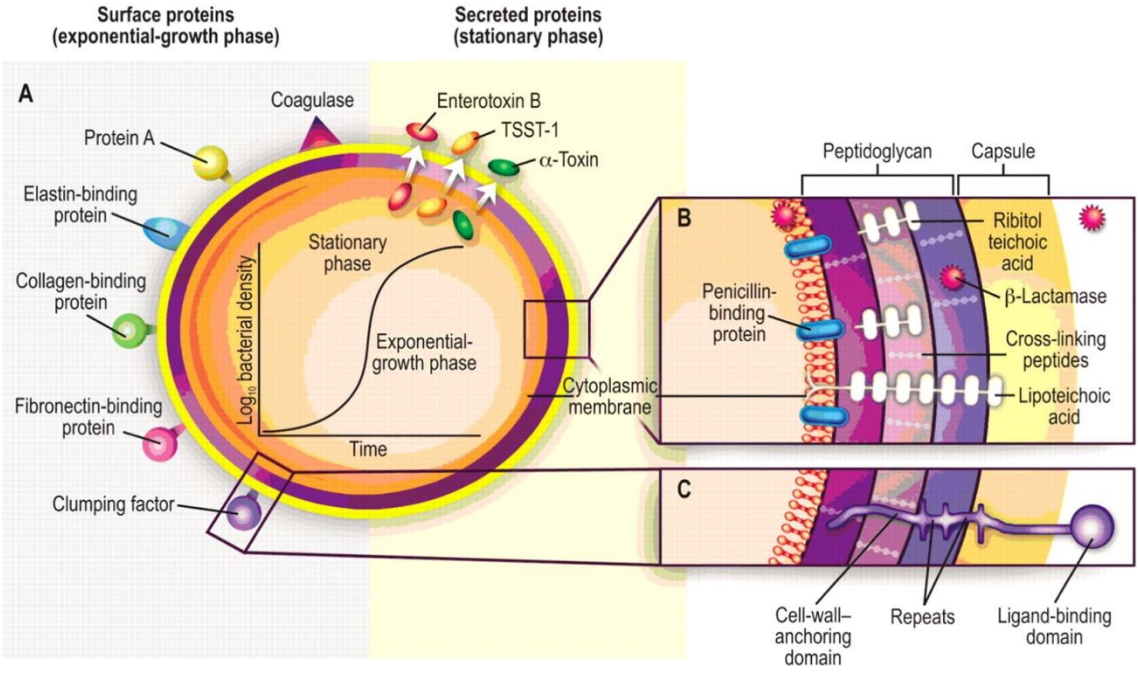


**Figure 6:** Pathogenic factors of *S. aureus*, with structural and secreted products both playing roles as virulence factors. (A) Surface and secreted proteins. (B, C) Cross-sections of the cell envelope. TSST-1: toxic shock syndrome toxin 1 (18).

Once a determined surface has been conditioned by proteins or other molecules present in the environment, the biofilms can form on virtually any surface. The microorganisms attach to the surface and in time begin to release DNA, proteins and polysaccharides (17). By releasing these molecules, the microbes became more stuck and stable on the surface. Over time, the biofilm

increases its thickness and maturity and the microorganisms start to reproduce and secrete additional molecules. In the end, the result is a complex and dynamic microorganism community. Within the biofilm, the microorganisms become protected from many harmful agents, such as antibiotics, UV light and other antimicrobial agents. The resistance of biofilm microorganisms frequently causes serious illness and failure of medical devices as they became difficult to eradicate (17).

*Staphylococcus spp.* is able to produce a multilayered biofilm embedded with a glycocalyx or slime layer (12). The development of the glycocalyx occurs on devitalized tissues (e.g. bone) and on implanted medical devices, leading to infection. The presence of these implants is a risk factor for the devolvement of infection because medical devices adsorb host proteins on their surface immediately after implantation. These proteins are excellent sources for the attachment of microorganisms that were introduced or remained after surgery (12). After the attachment to the surface, the bacteria start to form the glycocalyx. Considering all the characteristics mentioned above, it is clearer why *S. aureus* are very difficult bacteria to eradicate and continues to prevail with such high occurrence.

### 1.2.4. Current treatment

Despite the improvements in the treatment of osteomyelitis, it is still very difficult for orthopedic surgeons to control this infection, particularly when it is caused by resistant strains of *S. aureus* (20). The prosthetic devices are very susceptible to infections that are caused mainly by *S. aureus* or coagulase-negative staphylococci (e.g. *S. epidermidis*) (19). In a significant number of cases, the prosthesis must be removed and replaced by another, which implies a significant impact in terms of morbidity, mortality and medical costs (21).

The treatment for osteomyelitis includes an antimicrobial therapy, removal of the infected and necrotic tissue with management of resultant dead space and, when necessary, the stabilization of bone (11). The antimicrobial therapy for osteomyelitis involves a long parenteral administration of antibiotic (10). The choice of antibiotic should be determined by microbial cultures and susceptibility results. If this information is not available, a broad spectrum empiric antibiotic should be administered. However, if clinically possible, it is recommended to delay the antibiotic administration until microbial cultures and susceptibility results are available (13).

Glycopeptides are known to be effective antibiotics against *S. aureus* and they are frequently used for bone and joint infections. However, the existence of some staphylococci resistant to glycopeptides was already reported (22). The recommended treatment for osteomyelitis caused by *S. aureus* is the long and parenteral administration of penicillin or vancomycin. But this treatment requires a prolonged stay in hospital, which implies higher economical costs. In addition, the parenteral administration for this treatment involves the use of catheters, which have their own

infection-associated risks and problems (10). On the other hand, multi-resistant strains may appear when a long treatment using the same antibiotic is performed, as observed for penicillin and vancomycin (23). Moreover, the infection causes bone malformations that make more difficult the diffusion of some antibiotics, particularly vancomycin, even if higher doses are used (20). When antibiotic failure occurs, it is recommended to perform surgery (13).

In conclusion, the treatment of osteomyelitis is difficult, long and frequently invasive. Therefore, it is important to develop a strategy to improve the treatment. One possible approach would be using a sustained drug release vehicle composed by a calcium phosphate and collagen, as they both mimic natural bone tissue and are capable to induce bone tissue regeneration (24).

## 1.2.5. Vancomycin

Vancomycin is a glycopeptide antibiotic with a molecular weight of approximately 1450 Da (25) and it is very effective against gram-positive bacteria, namely *S. aureus* (Figure 7) (26). It was first isolated in 1950 and it was used for the first time in therapeutics in 1959 (27). Structurally, this glycopeptide is composed by seven amino acids (28) and normally forms a dimer (26). In the early times after its discovery, vancomycin was not very used because there were other antibiotics considered less toxic and similarly effective.

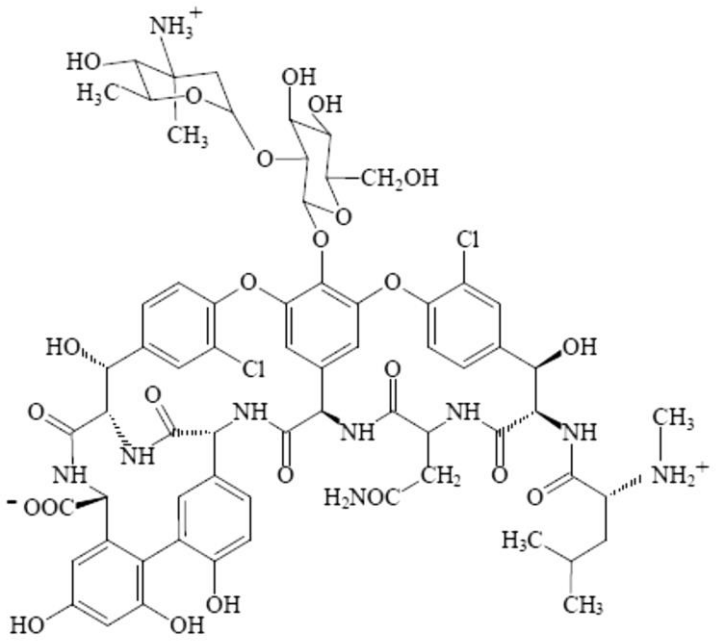

**Figure 7:** Chemical structure of vancomycin (27).

But the appearance of resistant pathogens, such as MRSA and *Streptococcus pneumoniae*, caused a more frequent administration of this antibiotic (29). Vancomycin acts on bacteria by interfering with the synthesis of the peptidoglycan cell wall (26). This antibiotic binds specifically to the C-terminal D-Ala-D-Ala sequence of the pentapeptide of lipid II. The latter is one of the key molecules for bacterial cell wall synthesis. Lipid II is essential for the transport of cell wall subunits across the cytoplasmatic membrane of the bacteria. The binding of vancomycin to lipid II prevents the adhesion of penicillin-binding proteins (PBPs). PBPs are responsible for the polymerization and integration of the peptidoglycan into the cell wall. As a result, the cell wall synthesis is inhibited, leading to cell dead (30).

Considering its physicochemical properties, vancomycin is classified as an acid antibiotic (31). Its isoelectric point (pI) is 8.3, being cationically charged at physiological pH (32). It was shown that for a pH=2, the vancomycin net charge is approximately +2. Increasing the pH to 7.4, the net charge decreases to +0.7 (33, 34). The referred physicochemical properties are important parameters to design effective therapeutic strategies (35). Vancomycin has many advantages when compared to other antibiotics. First, it was observed that vancomycin is one of the least cytotoxic antibiotics and did not significantly affect the osteoblast number and ALP production, even when higher concentrations were used. Therefore, vancomycin is an appropriate antibiotic to be used in bone applications (36). In addition, vancomycin has a standardized low minimum inhibitory concentration (MIC) of 1 µg/mL for *S. aureus* (37, 38), but this value may vary according to bacterial strain (39), pH and inoculum size (40). In spite of being an effective antibiotic against *S. aureus*, in 2002 a clinical isolate of vancomycin-resistant *S. aureus* (VRSA) was identified (41).

### 1.2.6. Drug release profile

Considering the local prevention of bacterial infections associated with orthopedic implants, the success of antibiotic delivery systems is related with the drug release profile. It is crucial to maintain a controlled release profile during a certain period. If the entire dose is rapidly released, it can be delivered before the bacteria are eradicated. However, if the release profile is too slow, the infection may develop further. In fact, if the levels of antibiotic are maintained below the MIC, a bacterial resistance may appear. In order to treat or prevent bone infections, it is recommended to have an initial burst release of antibiotic, followed by a sustained release to a complete eradication of the pathogen agent (21). However, the initial burst release must be controlled and, if possible, remain below the minimum toxic concentration (MTC). The achievement of this therapeutic window is the one of the main challenges of numerous drug delivery approaches (37).

## 1.3. Biomaterials for osteomyelitis

Considering bone infections, it would be beneficial to have a local drug delivery system (DDS) that could release the antibiotic and induce osteogenesis (42). Therefore, the calcium phosphates are promising materials, as they are useful for bone tissue regeneration and there were already reports indicating that calcium phosphates are efficient materials for DDS (21).

### 1.3.1. Hydroxyapatite

Calcium phosphate-derived materials are amongst the most successful materials for bone applications. These materials are bioactive and they have the capacity of adsorbing many different molecules on their surface, which makes them appropriate as DDS (43). The most used calcium phosphate is HA ($Ca_{10}(PO_4)_6(OH)_2$) (Figure 8). HA has a hexagonal structure (44, 45) and a stoichiometric Ca/P ratio of 1.67, which is very similar to that found in bone apatite (44, 46, 47). Due to this similarity between HA and mineralized bone, HA possesses a high affinity to hard tissues as it forms chemical bonds with the host tissue (44). Therefore, HA is been frequently used in medicine in implants for hard tissues substitution, i.e. teeth and bones. Lately, HA has been used in other biomedical applications, such as drug release systems. HA has been used in a variety of forms such as powders, granules, dense and porous blocks, thin and thick films. The use of granules is advantageous in cases of bone defects or hollows of irregular shapes (48), as happens in patients with osteomyelitis (10).

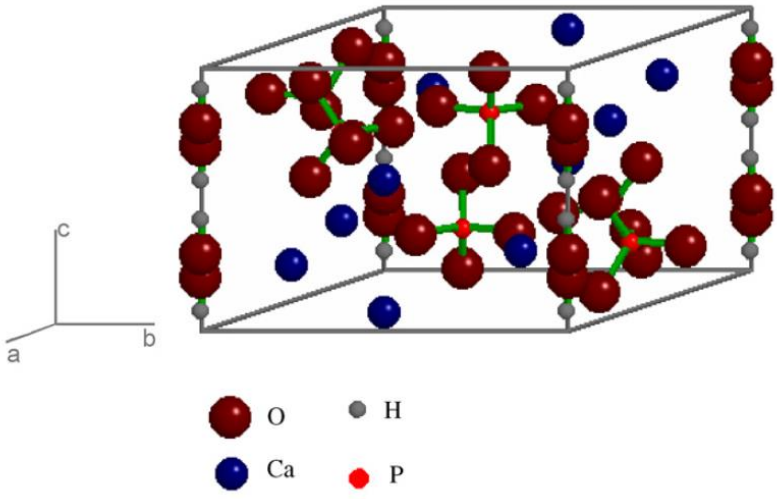


**Figure 8:** The unit cell of hydroxyapatite (45).

HA has other properties such as bioactivity, biocompatibility, solubility, sinterability and adsorption capability. These characteristics can be adapted over wide ranges by controlling the particle composition, particle size and morphology (49). The crystalline sizes of HA have been used to explain its bioactivity. It was reported that a higher number of differentiated osteoblasts and higher ALP activity were observed on sintered HA compared with non-sintered HA (47). As HA possesses a high level of biocompatibility, it has been chosen to produce dense and porous bioceramics (49). Another important characteristic of HA is its stability, compared to other calcium phosphates. Thermodynamically, HA is the most stable calcium phosphate compound at temperature, pH and composition of human physiological fluids (44). Although HA has an attractive bioactivity and biocompatibility, its use has been limited due to poor mechanical strength (49-51).

On the other hand, the mechanical properties of HA have been improved by the combination of this calcium phosphate with polymers, such as collagen. When combined with HA, the ductile properties of this polymer can help to increase the poor facture toughness of HA. Moreover, the stability of collagen is increased with the addition of calcium phosphate compounds (52). Independently from each other, it is known that HA and type I collagen are able to enhance osteoblast differentiation. However, when combined as a composite, they indicate to accelerate osteogenesis. Therefore, a HA/collagen composite should exhibit not only improved mechanical properties, but also adequate biological properties (52).

#### 1.3.1.1. Nanohydroxyapatite

The microscale HA production techniques have been the most frequently reported and extensively used. However, the nanotechnology had a tremendous development in the last years and nanohydroxyapatite (nanoHA) has been synthesized and studied to improve the performance of HA. Due to the large surface to volume ratio and higher surface reactivity, the nano-sized HA present improved performance. As bone possesses an hierarchical structure with nanometer dimensions, the nanoHA is a promising ceramic to mimic this tissue (48). Comparing nano-sized HA with the traditional micro-sized HA, the first one has special properties that can control protein adsorption and osteoblast adhesion, such as grain size, pore size and wettability (53, 54). In addition, nanoHA also enhances osteoblast functions like proliferation, calcium containing mineral deposition and ALP synthesis (53). A possible suggestion for this is that nanoHA is more similar to bone apatite in size and morphology, when compared with micro-sized HA (55).

NanoHA has been studied as potential material for DDS, particularly for vancomycin (20, 56). The combination of this material and vancomycin can be a promising strategy to be applied in cases of osteomyelitis.

## 1.3.2. Collagen

Collagen is a natural polymer synthesized by fibroblasts and osteoblasts among other cells (57), which has been increasingly used in tissue engineering and repair (52, 58, 59). It is considered the most abundant protein on earth, has excellent mechanical properties and is an example of a hierarchical biological nanomaterial (60). This polymer has an important role in the formation of tissues (58) such as bone (Type I), cartilage (Type II) and in blood vessels (Type III) (1).

The collagen fibers are formed by tropocollagen subunits (Figure 9). Each subunit has approximately 280 nm long and 1.5 nm in diameter (1). The tropocollagen molecules are constituted by three polypeptide chains named α-chains, which are enfolded around each other, forming a triple helix. One α-chain is composed by approximately one thousand amino acid residues and every third amino acid is a glycine. Due to its small size, it is believed that glycine allows a closer association of the three α-chains. The majority of the remaining amino acids are proline, hydroxyproline and hydroxylysine. The latter binds the tropocollagen molecules to each other, allowing the formation of fibrils. The three α-chains are held together by the hydrogen bonds of hydroxyproline (1, 5, 60).

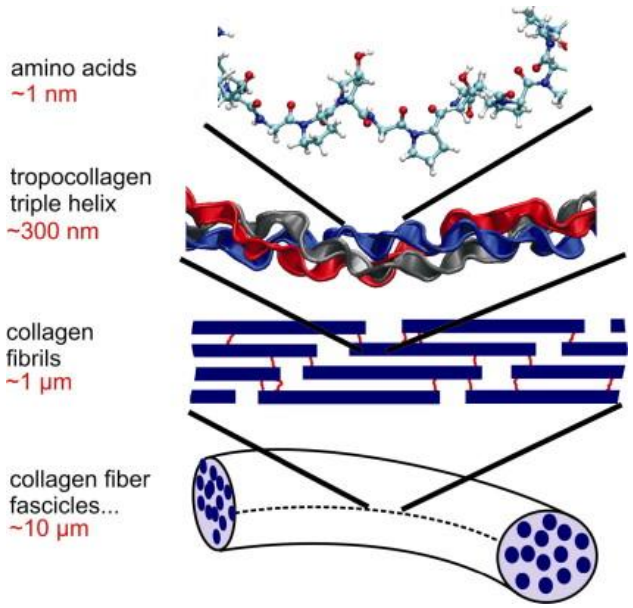


**Figure 9:** Schematic view of some of the hierarchical features of collagen (60).

Collagen is being commonly used in biomedical applications. The main reason why collagen has been so useful in biomedical applications is because it can form fibers with improved strength and stability through its crosslinking and self-aggregation. In addition, collagen has other important characteristics that make it more adequate to interact with the body, when compared to other natural or synthetic polymers. Comparing with natural polymers like gelatin, collagen possesses biodegradability, better

biocompatibility and weak antigenicity. Besides, collagen is nontoxic, can be solubilized into aqueous solution and is relatively stable since it is the primal structural protein in the body. However, collagen can be degraded by enzymes such as collagenase. The biomedical applications of collagen include surgical sutures, substitutes for artificial blood vessels and valves, matrices for cell cultures and vehicles for drug delivery (58).

Considering collagen as DDS, it has been studied to treat, for example, tissue infections and cancer. In both cases, the collagen matrix was able to maintain a sustainable release of drugs (58). Therefore, collagen seems to be a valuable material to be applied in a DDS.

### 1.3.3. HA/collagen composite

Collagen has already been tested for the improvement of HA mechanical and biological properties. In fact, the combination of these two materials is probably the most direct approach to obtaining a real bioactive artificial bone material, as it has a similar composition, nanostructure and biological response to bone (61).

The materials alone have many advantages such as biocompatibility and non-toxicity. In addition, they can inhibit the growth of bacterial pathogens, the main cause of infection in prosthesis (52). As a composite, it was already proved that the combination of HA and collagen has valuable advantages, such as proper degradation rate as a scaffold for bone repair and improved adhesion of osteogenic cells *in vitro*. In addition, the use of this composite as a DDS has already been studied, particularly for the cases of osteomyelitis, and a sustained release of the drug was reported combined with new bone formation and proper vascularized connective tissue, rich in cells and collagen (24). Therefore, the use of this type of composite as a DDS for the treatment of osteomyelitis can be promising, as it would not only release the drug, but also improve new bone formation conditions at the site.

### 1.3.4. Heparinized materials

Heparin is one of the components of ECM (62) and its structure is a mixture of branched glycosaminoglycans and it acts as an antithrombotic agent, inhibiting the blood coagulation (63, 64). It is known that heparin has affinity to bind to several proteins, including growth factors and collagen (65, 66). The structural characteristics of heparin suggest that the peptide sequences rich in basic amino acids, particularly lysines and arginines, can interact with the negatively charged groups of heparin, sulfur and carboxylic groups (Figure 10) (66). It was reported that heparin can be successfully incorporated on HA/collagen scaffolds during collagen crosslinking. In the latter reaction, the carboxylic group of heparin reacts with an amino group of collagen, resulting a covalent binding between the two molecules. In the same study it was also reported that the heparinized scaffold was

able to perform a sustainable release of bone morphogenetic protein-2 (BMP-2) (65). Therefore, immobilizing heparin on biomaterials may improve the performance of a DDS, performing a sustainable release. The combination of heparin with antibiotics has been tested to improve the performance of catheters (67, 68), namely with vancomycin (69). Therefore, the used of a heparinized nanoHA/collagen composite would be beneficial in cases of osteomyelitis to achieve a sustainable release of vancomycin and, simultaneously, induce bone regeneration.

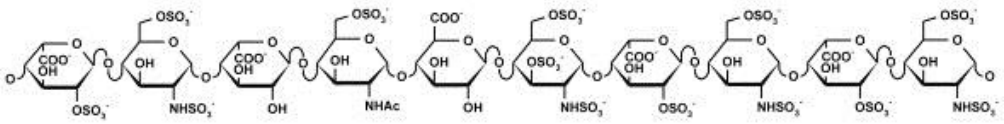

**Figure 10:** Heparin structure (70).

# Chapter 2: Materials and methods

## 2.1. Materials preparation

### 2.1.1. Production of nanoHA granules

To obtain nanoHA granules, scaffolds were prepared using polyurethane (PU) sponges (Recticel, Belgium) as a template that were impregnated with nanophased hydroxyapatite (nanoHA) slurry, using PU sponge impregnation method described elsewhere (48). The slurry was prepared with 5 g of nanoHA powder (highly pure spray-dried powder with an average particle size of 5.0 ± 1.0 µm, nanoXIM·Hap202, Fluidinova SA, Portugal), 4.4 mL of ultra-pure water and 200 µL of dispersive agent (DA) Dolapix CE64 (Zschimmer & Schwarz, Germany). Two other volumes, 150 and 250 µL, of DA were also tested. The impregnated sponges were dried at 37 °C in the oven for approximately 30 min and then heat-treated in a sintering furnace (Thermolab). The heat treatment cycle used was as follows: heating rate of 1 °C/min till 600 °C with 1 h plateau followed by a heating rate of 4 °C/min till 830 °C with 1 h plateau. After the heat treatment, the samples were cooled inside the furnace. Subsequently, granules were obtained by crushing in a mortar the sintered scaffolds. NanoHA granules were obtained using sieves with sizes between 1.18 and 1.70 mm, resulting in granules with sizes between those two values.

### 2.1.2. Collagen inclusion and crosslinking within nanoHA granules

A 0.5 % (w/v) collagen solution was prepared by dissolving Type I collagen (Bovine Achilles tendon, Sigma-Aldrich) overnight in HCl (0.01 M, pH=2) at 4 °C. The solution was then homogenized for 3 h using an Ultra Turrax (T25 D, IKA®) at 10000 rpm on ice. To assess the influence of collagen concentration on its distribution on nanoHA granules, several dilutions of 0.5 % collagen solution were prepared (0.05, 0.10, 0.15 and 0.25 %). The nanoHA granules were spread on petri dishes and a single drop of collagen solution was applied in each granule. Finally, the nanoHA granules were placed in a vacuum oven (Binder, Germany) at room temperature (RT, 25 °C) for 48 h to allow collagen to penetrate the granules.

Collagen chemical crosslinking was performed using *N*-(3-dimethylaminopropyl)-*N*'-ethylcarbodiimide (EDC, Aldrich) and *N*-hydroxysuccinimide (NHS, Fluka). Therefore, 27.6 mg of EDC and 10 mg of NHS were dissolved on 12 mL of 2-mofpholinoethane sulfonic acid (MES buffer, 0.05 M, pH=5.4, Sigma). The reaction was performed during 2 h at 4 °C. After the crosslinking reaction, the

solution was removed and the samples were washed 3 times with MES buffer and dried overnight in a vacuum oven.

### 2.1.3. Collagen crosslinking and heparin immobilization

Considering heparinized nanoHA/collagen granules, the collagen crosslinking and heparin immobilization were performed simultaneously. Consequently, 27.6 mg of EDC, 10 mg of NHS and 240 mg of heparin (Heparin sodium salt from porcine mucosa, Sigma) were dissolved in 12 mL of MES buffer (0.05 M, pH=5.4, Sigma). The reaction was performed during 2 h at 4 °C. Afterwards, the granules were placed in phosphate buffer saline (PBS, pH=7.4) for 2 h to stop heparin immobilization. PBS was then removed and the granules were washed 6 times during 4 h with 2 M NaCl, 4 times during 6 h with 4 M NaCl and 3 times during 8 h with ultra-pure water. After the washing steps, the heparinized nanoHA/collagen granules were dried overnight in a vacuum oven at RT.

## 2.2. Granules characterization

### 2.2.1. Scanning Electron Microscopy (SEM)

Scaffolds and granules morphology as well as collagen distribution and chemical characterization were studied using SEM and Energy-dispersive X-ray Spectroscopy (EDS) (FEI Quanta 400 FEG ESEM/EDAX genesis X4M) with an acceleration voltage of 15 kV. Previously, the samples were fixed with Araldite$^{TM}$ on the aluminum sample holder and sputter coated with a Au/Pd alloy thin film for 90 to 110 s (SPI Module Sputter Coater) to yield them electrical conductivity.

### 2.2.2. X-Ray Micro-Computed Tomography (Micro-CT)

Three dimensional (3D) structure of nanoHA and nanoHA/collagen granules was accessed with X-ray Micro-Computed Tomography (Micro-CT) Skyscan 1072 scanner (SkyScan, Kontich, Belgium) in high-resolution mode of 6.69 µm x/y/z. One nanoHA granule and three nanoHA/collagen granules were scanned for approximately 1 h each using a pixel size of 3.29 µm. The energy and current of the X-ray source was 57 kV and 175 µA, respectively. 250 slice images (two dimensional, 2D) were considered and converted into binary images using a lower grey threshold of 60 and an upper grey threshold of 255, in order to distinguish ceramic material from pore voids. The slide images were assembled to yield 3D images and reveal quantitative morphological parameters. For 2D and 3D image processing and visualization, two SkyScan softwares were used: CT Analyzer v.1.12.0.0 to obtain the morphological data and CTVox to create the 3D models of the granules.

### 2.2.3. Attenuated Total Reflectance Fourier Transformed Infrared Spectroscopy (ATR-FTIR)

The chemical composition of non-sintered nanoHA powder, nanoHA, nanoHA/collagen and heparinized nanoHA/collagen granules and crosslinked collagen was assessed with ATR-FTIR. For that purpose, it was used a FTIR spectrometer (Perkin Elmer 2000, U.S.A.), with a resolution of 4 $cm^{-1}$, a frequency region from 400 to 4000 $cm^{-1}$ and 100 scans were accumulated per sample. To perform ATR-FTIR, a Split Pea accessory (Harrick Scientific Corporation, U.S.A.) was used containing a silicon hemispherical crystal.

## 2.3. Vancomycin adsorption and releasing from granules

### 2.3.1. Vancomycin loading

20 mg of granules were placed in eppendorf tubes and submerged in 1 mL vancomycin solution (Vancomicina Combino, Pharm) with a concentration of 25 mg/mL (pH=4). Vancomycin adsorption onto granules was performed at 37 °C and 120 rpm in the orbital shaker (KS 4000 IC, IKA®) for 24 h.

### 2.3.2. Release kinetics and bioactivity

After vancomycin loading, the supernatant solution was removed and the granules were transferred to new eppendorf tubes and 1 mL of PBS (pH=7.4) was added. Eppendorf tubes were placed in the orbital shaker at 37 °C and 120 rpm. To determine the vancomycin release from the granules, 200 µL of solution were withdrawn and replaced by fresh PBS solution after 0.25, 0.5, 1.5, 2.5, 3.5, 24 h and from then onwards every 24 h up to 360 h. Control experiments using antibiotic-free ceramic samples were performed under the same experimental conditions (negative control). All tests were performed in triplicate. The removed solution was centrifuged for 5 min and 14000 rpm to avoid particles in suspension. Vancomycin concentration was determined by molecular absorption spectroscopy at 280 nm using a spectrophotometer (Lambda 35 UV/Vis Spectrometer, Perkin Elmer, U.S.A). The samples were subsequently frozen at -20°C to perform microbiology assays.

Vancomycin bioactivity of the eluted samples was tested using the diffusion method (71). Nutrient agar (NA, Liofilchem, Italy) plate inoculated with *Staphylococcus aureus* (*S. aureus*) ATCC 25923 was used to create a suspension on NaCl with 1.5 x $10^8$ colony-forming units (CFU)/mL, which equals to 0.5 Mcfarland equivalence turbidity standard in ambient light, using a densitometer (BioMerieux, France). 1.5 mL of bacteria suspension was incorporated on 250 mL of nutrient agar heated at 50 °C. 20 mL of nutrient agar was poured on sterile plates and left at RT to dry. 70 µL of each sample solution containing vancomycin released from granules was placed into 10 mm stainless steel

cylinders inserted into different areas of the agar. The plates were left at RT for 30 min to allow vancomycin diffusion into the agar and then incubated at 37 °C. After 18 h of incubation, the inhibition zone diameters were measured.

Since the diffusion method was proved to be unsuitable for this work, vancomycin bioactivity was also assessed using broth microdilution method, which is normally used to determine the MIC (72). Therefore, *S. aureus* ATCC 25923 were grown on nutrient broth (NB, Liofilchem, Italy) for 24 h at 37 °C and 120 rpm. From that bacterial suspension, an inoculum was taken and adjusted to an absorbance (640 nm) of 0.2, corresponding to $3.8x10^8$ CFU/mL. Afterwards, 96-well plates were filled with bacteria suspension (180 µL) and with the released vancomycin (20 µL). 8 wells were used for each time point analysed. NB medium without bacteria and bacteria suspension without vancomycin were used as controls. The plates were incubated for 24 h at 37 °C and 120 rpm. After incubation, the absorbance was measured at 640 nm using a microplate reader (Spectramax M2e, Molecular Devices, Inc.). The absorbance values were converted to total number of bacteria/mL using a calibration curve.

## 2.4. *S. aureus* adhesion on granules

### 2.4.1. Quantification of adherent *S. aureus*

The adherence of *S. aureus* on three type of granules was studied to see if bacteria have some tendency to migrate to one type of granules rather than another. For that, *S. aureus* ATCC 25923 was cultivated on tryptic soy broth (TSB, Difco, USA) for 18 h at 37 °C. The bacterial solution was harvested by centrifugation for 5 min at 18 °C and 2000 rpm and washed twice and resuspended in on NaCl to create a suspension with 1.5 x $10^8$ CFU/mL, which equals to 0.5 Mcfarland equivalence turbidity standard in ambient light, using a densitometer (BioMerieux, France). To allow bacterial adhesion to granules, 20 mg of granules were placed in a glass tube with 1 mL of bacterial suspension and incubated in a gently shaking water bath at 37 °C for 1 h. The experiment was performed in triplicate. After incubation, each sample was washed 2 times with NaCl to remove non-adherent bacteria. Then, 5 mL of NaCl were placed in each tube and sonicated for 1 s at 20 KHz using a sonicator (Sonoplus HD 2200, Bandelin, Germany) with a MS 73 probe. The sonicated solutions were used to make serial dilutions and these were placed onto nutrient agar culture plates and incubated at 37 for 18 h. Afterwards, the number of adherent bacteria was counted and the number of CFU/$mm^2$ was determined.

### 2.4.2. Visualization of adherent *S. aureus*

*S. aureus* was fixed using 1.5 % glutaraldehyde (v/v) (Agar) in 0.14 M cacodylate buffer (Merk) during 10 min and dehydrated in graded series of ethanol solutions. The samples were dried overnight at RT. Adherent *S. aureus* on granules were visualized using SEM as previously described.

## 2.5. Osteoblast culture

MC3T3-E1 cells, an osteoblastic cell line from mouse calvaria, were grown in alpha minimum essential medium (α-MEM, Gibco), supplemented with 1 % penicillin-streptomycin (Gibco) and 10 % fetal bovine serum (FBS, Invitrogen). Cells were incubated in a humidified environment at 37 °C and 5 % of $CO_2$. Vancomycin adsorption on granules was performed as mentioned above. Granules were placed in 96-well plates and cells were seeded using a density of $5x10^4$ cells/mL. Cells were cultured during 21 days and medium was changed three times a week. As control, cells were cultured on tissue culture polystyrene (TCPS) with the same conditions used for the granules. For each condition, six replicates were used for the resazurin assay.

### 2.5.1. Metabolic activity

The non-toxic Alamar Blue (Resazurin) dye was used to determine the metabolic activity of MC3T3-E1 cells. The blue non-fluorescent dye is metabolized by cells, converting to a reduced pink fluorescence dye (73). Therefore, 10 % (v/v) of resazurin was added to the medium and incubated for 4 h at 37 °C and 5 % of $CO_2$. Afterwards, 100 µL were transferred into a black 96-well plate and fluorescence was measured at 530 nm excitation and 590 nm emission wavelength with a fluorescence reader (SynergyMix, BioTek) using Gen5 1.09 Data Analysis Software. These measurements were made at 24 h, 4, 7, 14 and 21 days of culture.

### 2.5.2. Cell Morphology

#### 2.5.2.1. Confocal Laser Scanning Microscopy (CLSM)

Granules with seeded cells were washed twice with pre-heated PBS, fixed using 4 % paraformaldehyde (PFA) during 15 min and then washed twice with PBS. 0.1% Triton X-100 for 5 min was used to permeabilize cells and then incubated in 1 % Bovine Serum Albumin (BSA) at 37 °C for 30 min. After incubation, the staining of the F-actin filaments was performed using Alexa Fluor 594 Phalloidin (1:100, Molecular Probes A12379, Invitrogen) in 1 % BSA at RT for 20 min in dark. The samples were then washed twice with PBS. Cell nuclei were stained with a solution of Hoechst dye (1:1000, Sigma) in PBS at RT for 15 min in dark. Finally, the samples were washed twice with PBS and

one drop of Vectashield was added. The granules were placed in an appropriate dish to acquire images with a Leica SP5 Confocal microscope, using a 20x oil objective. The acquired images were processed with Leica Application Suite Version 2.6.0.

#### 2.5.2.2. Scanning Electron Microscopy (SEM)

Granules with seeded cells were rinsed with pre-heated PBS and fixed using 1.5 % gluteraldehyde (v/v) (Agar) in 0.14 M sodium cacodylate buffer (Merck) at RT for 30 min. The samples were washed twice with PBS and then dehydrated in graded series of ethanol solutions for 10 min each. Hexamethyldisilazane (Sigma) was added and the samples were dried overnight in the hood. Granules were visualized with SEM as previously described.

## 2.6. Statistical analysis

The statistical analysis was performed using the one-way analysis of variance (One-way ANOVA) followed by a post hoc Tukey test with a significance level of $p < 0.05$. The data analysis was done using GraphPad Software version 5.02 (GraphPad Software, Inc., U.S.A).

# Chapter 3: Results

## 3.1. Characterization of nanoHA and nanoHA/collagen granules

### 3.1.1. SEM

SEM was used to analyze the effect of the DA Dolapix CE64 on the morphology of the nanoHA scaffolds, as well as the granules morphology and collagen distribution on them. Figure 11 presents the results obtained for the optimization of the amount of Dolapix CE64 in the nanoHA slurry. The presence of macroporosity is visible for all different volumes of DA (Figure 11A, D and G). It was seen that the best condition for the scaffold synthesis is the use of 200 µL of DA in the nanoHA slurry (Figure 11D, E and F). When 150 µL of DA were used, it was observed that the structure of the scaffold was very brittle, showing many cracks along the pore walls (Figure 11A) and between nanoHA grains (Figure 11C). These scaffolds were also very fragile and did not have enough resistance to be transformed into granules. For 250 µL, the nanoHA grains did not have a normal round shape as they present some coalescence (Figure 11H and I). For the referred volume, the presence of microporosity is not as evident as for 200 µL of Dolapix CE64 (Figure 11E). Therefore, the use of 200 µL of DA is considered the best condition to produce the nanoHA slurry and create scaffolds with adequate morphology and resistance to be transformed into nanoHA granules.

After the optimization of the nanoHA slurry, the scaffolds were crushed and sieved. Among the available ranges of sieves, the ones between 1.18 and 1.70 mm were chosen as the granules with sizes in this range have adequate resistance and macroporosity. For smaller ranges, the granules obtained were too small, fragile and lacking macroporosity (Figure 12A and B).

Collagen inclusion was performed on nanoHA granules after determining their adequate size. Four different concentrations of collagen were tested (0.05, 0.10, 0.15 and 0.25 %) and Figure 13 illustrates the results obtained with SEM for the mentioned concentrations.

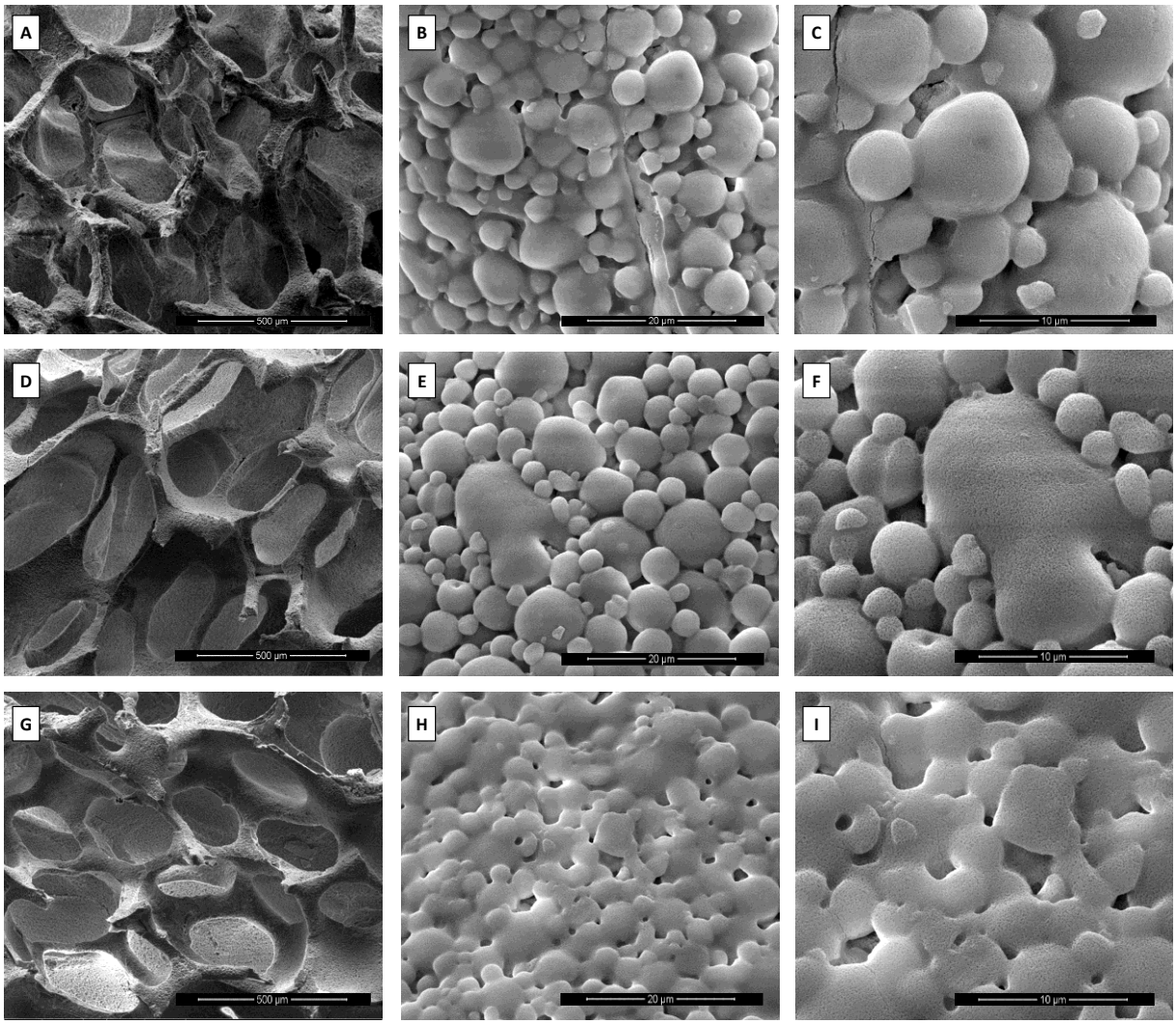


**Figure 11:** Morphology of nanoHA scaffolds produced with a slurry containing different volumes of DA. (A, B, C) 150 µL; (D, E, F) 200 µL; (G, H, I) 250 µL.

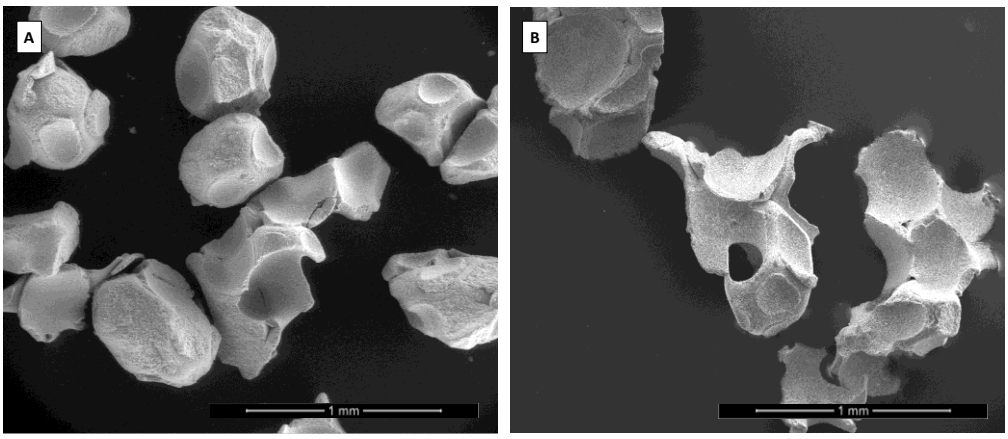


**Figure 12:** NanoHA granules. (A) 355-500 µm; (B) 500-850 µm.

It was shown that for the concentrations of 0.10, 0.15 and 0.25 % of collagen (Figure 13B, C and D), a layer of collagen was formed almost covering the nanoHA surface. As it is intended to produce a composite of both ceramic and polymer, the two types of material must be available to interact with molecules, bacteria and cells. Therefore, 0.10, 0.15 and 0.25 % of collagen are not adequate since they cover the ceramic surface. The ideal combination of the two materials was obtained using a 0.05 % collagen solution (Figure 13A). For this concentration, a fiber-like structure present along the nanoHA surface without completely covering was observed. Figure 14 shows some characteristics of the nanoHA/collagen granules. The presence of interconnective porosity between macropores (Figure 14A) and presence of microporosity (Figure 14 E) were observed. In addition, the collagen fiber-like structure is distributed on nanoHA with heterogeneous forms.

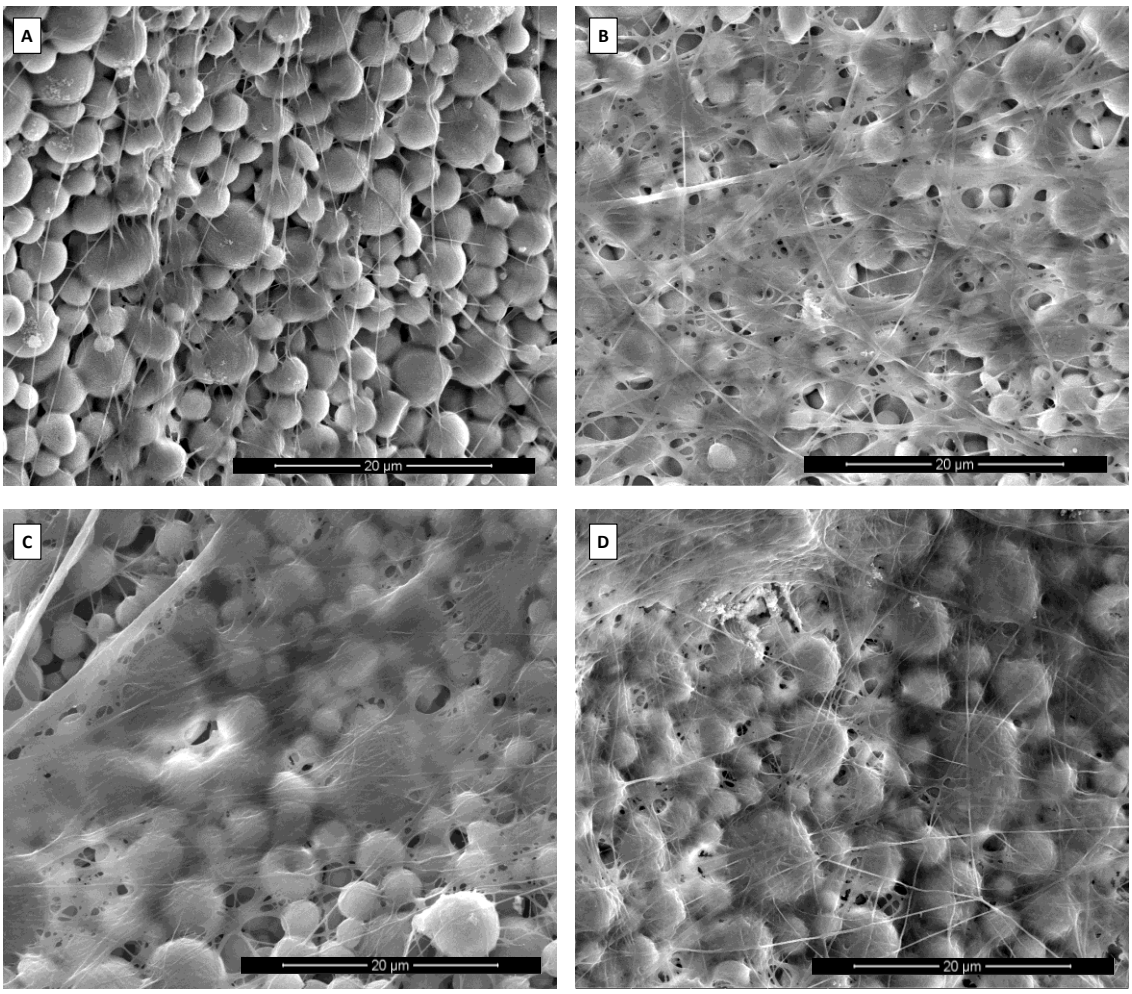


**Figure 13:** NanoHA/collagen granules produced with different concentrations of collagen. (A) 0.05 %; (B) 0.10 %; (C) 0.15 %; (D) 0.25 %.

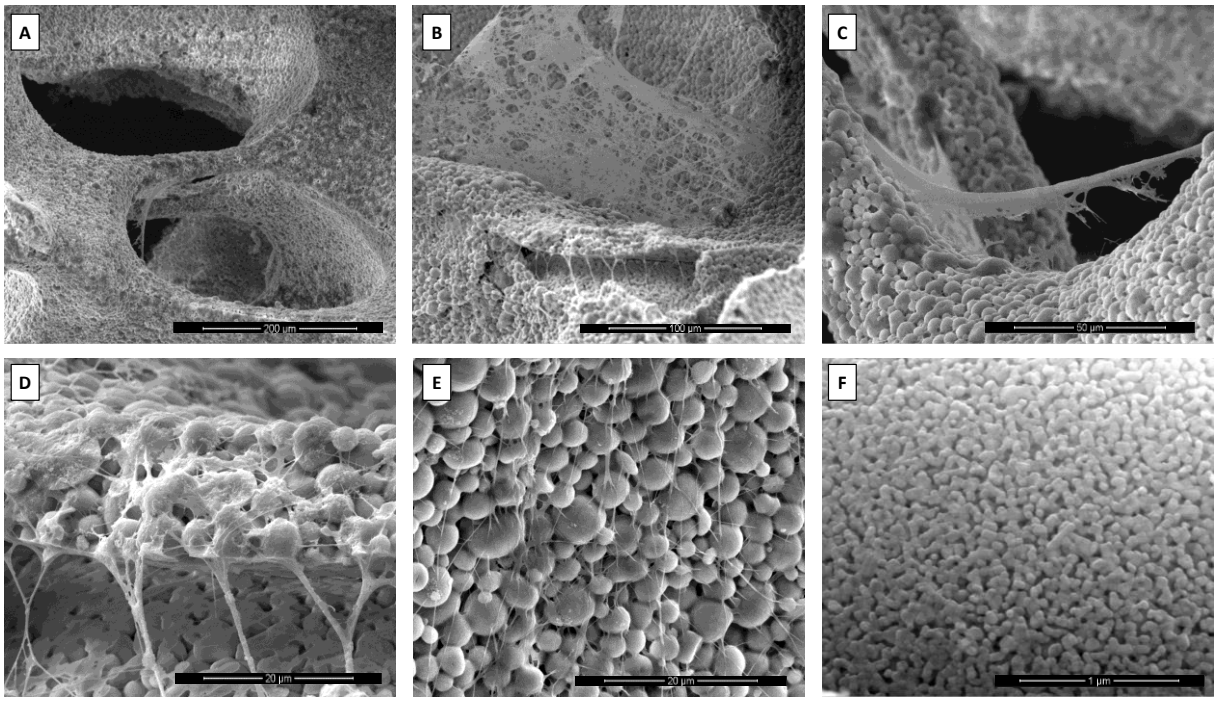


**Figure 14:** SEM images from nanoHA/collagen granules. (A) Presence of interconnective macroporosity; (B, C, D, E) Distribution of collagen in a fiber-like structure on nanoHA; (F) Presence of nanoporosity.

For example, collagen can form large fiber-like structures across a macropore (Figure 14B and C) and also forms smaller fibers between nanoHA grains (Figure 14D and E). Moreover, the presence of nanoporosity on the surface of nanoHA grains was evident (Figure 14F).

EDS analysis was also performed to chemically characterize the samples and determine the elements present on granules. For nanoHA granules, as expected it was detected the presence of calcium and phosphorus for the HA (Figure 15A). Gold and palladium were also detected, being associated to surface coating for SEM observation. Considering the EDS of nanoHA/collagen granules, the presence of calcium and phosphorus was also detected (Figure 15B). In addition, it was seen that carbon and oxygen were present in higher amounts than on nanoHA granules.

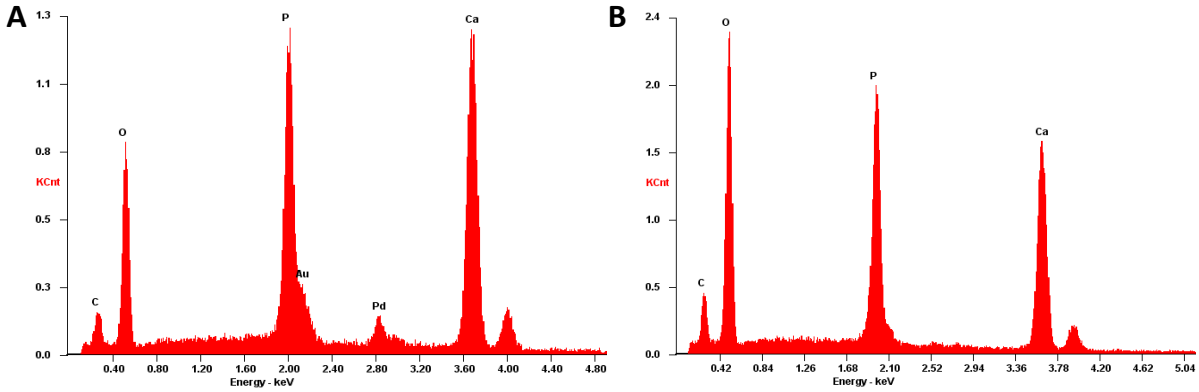


**Figure 15:** EDS analysis from granules. (A) NanoHA; (B) NanoHA/collagen.

## 3.1.2. Micro-CT

Micro-CT was used to assess the granules 3D structure and determine important parameters such as surface area, porosity and mean pore size (Table 2). The results obtained with this technique also sustained the results obtained with SEM, as they presented granules with interconnective macroporosity (Figure 16).

**Table 2:** Average porosity, surface area and mean pore size for nanoHA/collagen granules obtained by micro-CT

| Porosity (%) | Surface area ($mm^2$) | Mean pore size (µm) |
|---|---|---|
| **62.7 ± 1.5** | **26.6 ± 5.6** | **227.3 ± 7.2** |

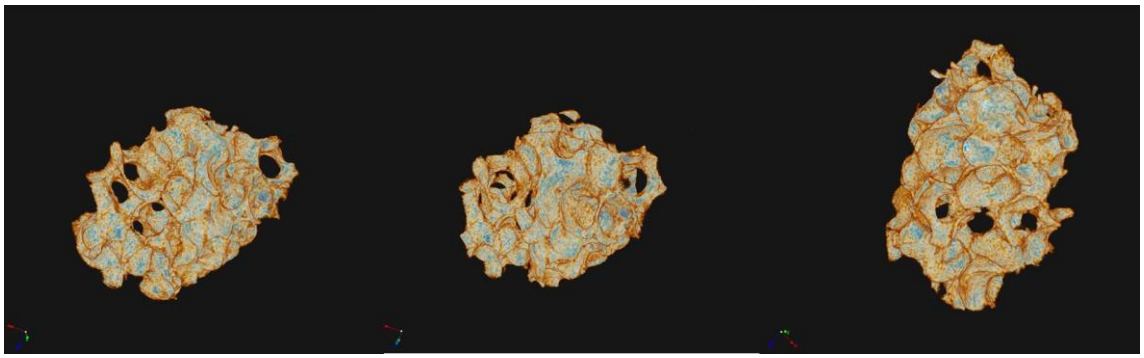

**Figure 16:** 3D micro-CT images from a nanoHA/collagen granule from different perspectives.

## 3.1.3. ATR-FTIR

To evaluate the chemical composition of the material, ATR-FTIR analysis was performed and is reported on Figure 17. Five different samples were analyzed: non-sintered nanoHA powder, crosslinked collagen, nanoHA granules, nanoHA/collagen granules and heparinized nanoHA/collagen granules. Considering the samples containing nanoHA, the peaks for the presence of the $PO_4^{3-}$ groups were obtained at 473, 565, 600, 962, 1028 and 1088 $cm^{-1}$. The bands at 630 and 3572 $cm^{-1}$ correspond to $OH^-$ vibrational and stretching modes, respectively. Table 3 indicates the obtained peaks for the samples containing collagen. The characteristic peaks for amide I (C=O stretching at 1600-1700 $cm^{-1}$), amide II (N-H deformation at 1500-1550 $cm^{-1}$) and amide III (N-H deformation at 1200-1300 $cm^{-1}$) are shown in Figure 17B (74). The crosslinked collagen has a broad band at 3200-3600 $cm^{-1}$ indicating the presence of adsorbed water on the material (48).

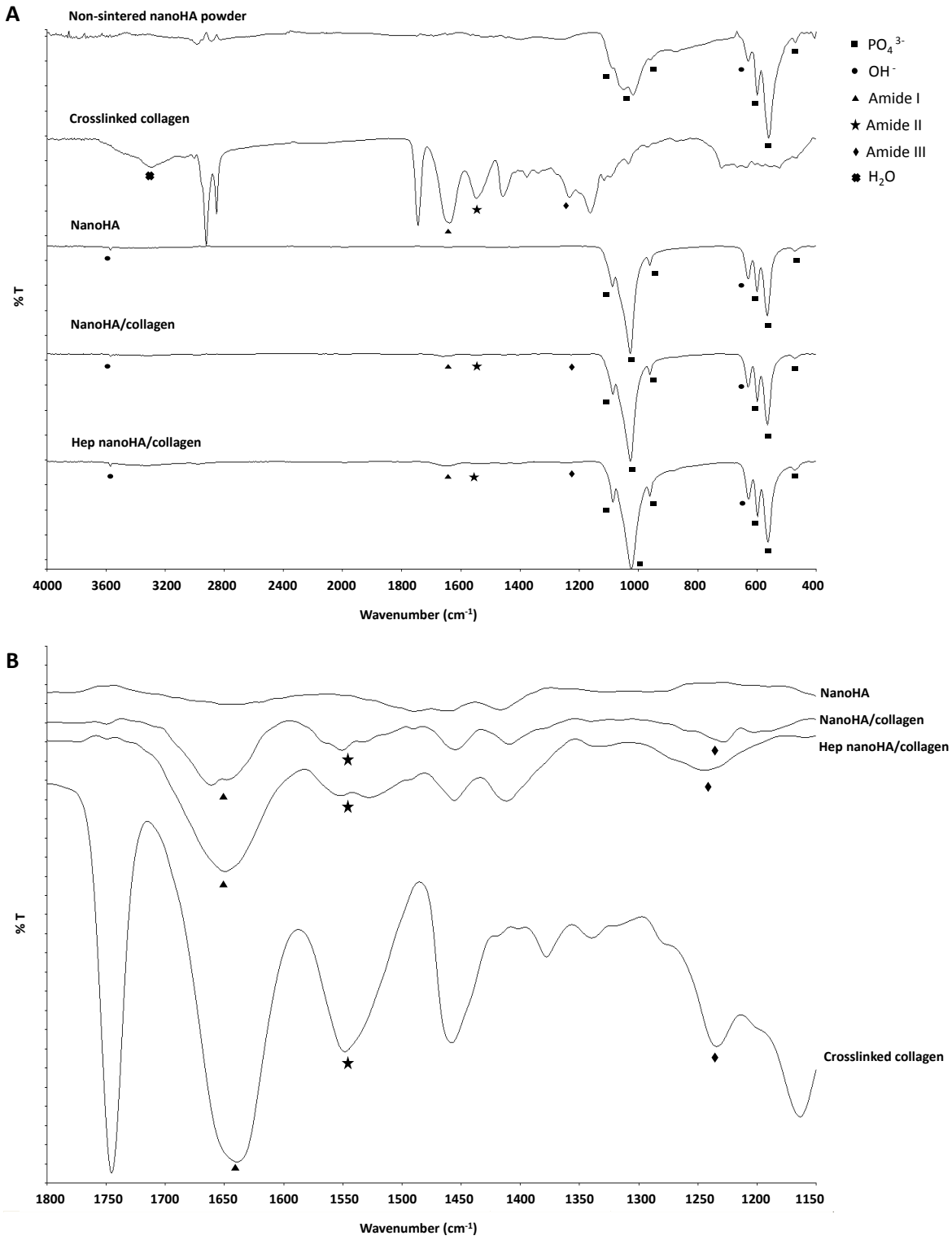


**Figure 17:** FTIR spectra of (A) Non-sintered nanoHA powder, crosslinked collagen, nanoHA, nanoHA/collagen and heparinized nanoHA/collagen granules; (B) Magnification between 1150-1800 $cm^{-1}$ for crosslinked collagen, nanoHA, nanoHA/collagen and heparinized nanoHA/collagen granules.

For the heparinized nanoHA/collagen granules, there was no different peaks present as heparin peaks are superimposed over collagen ones (75). However, it was observed that for the heparinized sample, the peak corresponding to amide I is more intense when compared with the non-heparinized sample possibly indicating the presence of heparin in the sample.

**Table 3:** Amide peaks obtained for crosslinked collagen, nanoHA/collagen granules and heparinized nanoHA/collagen granules.

| | Wavenumber ($cm^{-1}$) | | |
|---|---|---|---|
| **Material** | Amide I | Amide II | Amide III |
| Crosslinked collagen | 1639 | 1548 | 1237 |
| NanoHA/collagen | 1661 | 1550 | 1227 |
| Hep nanoHA/collagen | 1649 | 1550 | 1245 |

## 3.2. Vancomycin release from granules

The releasing of vancomycin from granules was studied for nanoHA, nanoHA/collagen and heparinized nanoHA/collagen granules. Figure 18 illustrates the releasing profile from the three different granules. Considering the nanoHA and nanoHA/collagen granules, vancomycin was released for 288 h and, for each time point, with no significant difference between these two types of granules. Regarding the heparinized nanoHA/collagen granules, the releasing of vancomycin for 360 h was measured, three more days than for the other two granules. Moreover, from 3.5 h of releasing, the amount of vancomycin released from the heparinized nanoHA/collagen granules was significantly higher, when compared to the nanoHA and nanoHA/collagen granules. The graphic with the cumulative released vancomycin (Figure 19) evidences the higher amount of vancomycin released from heparinized nanoHA/collagen granules. For the three different types of granules used, the determined released concentration present in each time point was always above *S. aureus* MIC (1 μg/mL) and bellow MTC (50 μg/mL) for vancomycin (37).

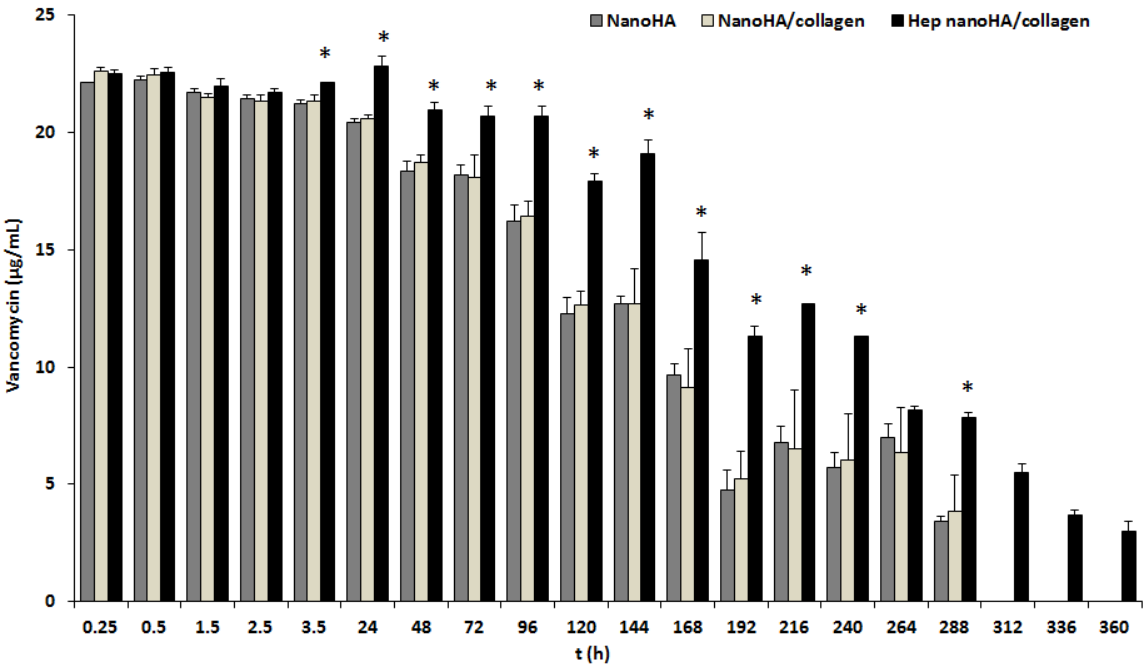


**Figure 18:** Vancomycin released from nanoHA, nanoHA/collagen and heparinized nanoHA/collagen granules as a function of time. The values correspond to the concentration present in each time point.* represents a statistical significant difference when compared to nanoHA and nanoHA/collagen granules for each time point ($p<0.05$).

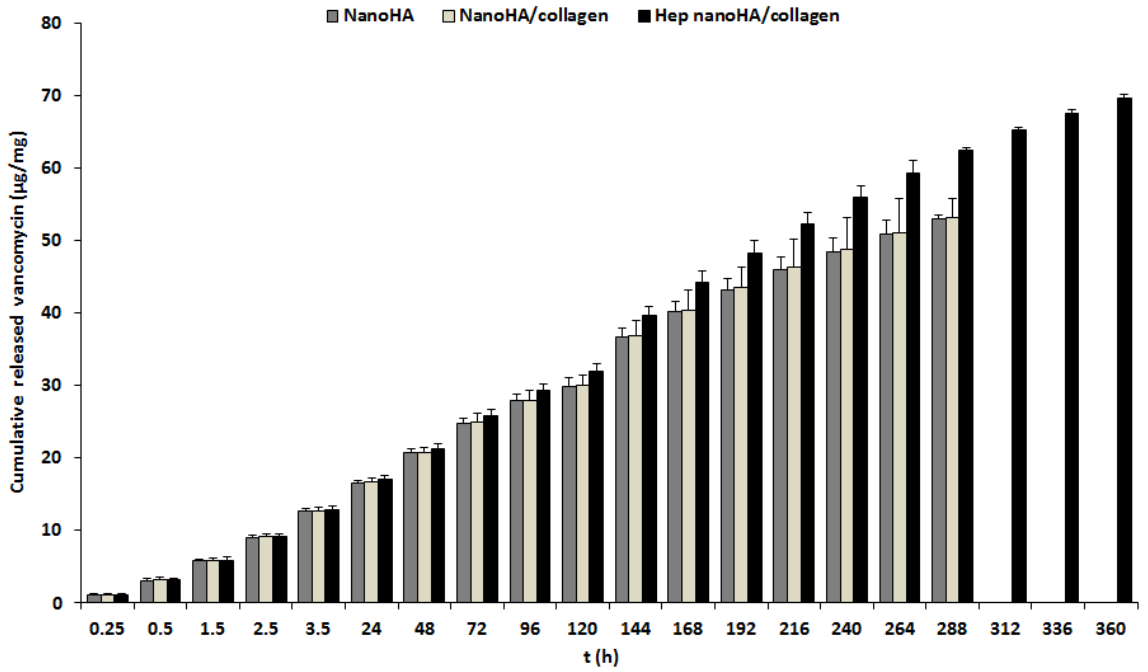


**Figure 19:** Cumulative release of vancomycin (µg of vancomycin/mg of granules) as a function of time.

## 3.3. Vancomycin bioactivity

For granules that presented the best vancomycin release profile (heparinized nanoHA/collagen), microbiology assays were performed to assess the released vancomycin bioactivity. In other words, these assays were performed to test if the antibiotic was still able to inhibit *S. aureus* growth. Firstly, the diffusion method was performed and three releasing time points were tested: 0.25, 24 and 120 h (Figure 20). For 0.25 and 24 h of vancomycin releasing, the bioactivity of vancomycin was confirmed, as inhibition zones were formed around the stainless steel cylinders, demonstrating that bacteria did not growth where the antibiotic was applied (Figure 20A, B, D and E). However, for 120 h of release, no inhibition zone was observed (Figure 20C and F). That fact could be related with loss of vancomycin bioactivity or probably due to the limit of detection of this technique. Thus, a higher mass of granules (50 mg) was used and the same releasing procedure was carried out to clarify the result. It was shown that for the referred time point, an inhibition circle is present for the 50 mg of granules (Figure 21B and D). Therefore, the concentration of vancomycin released from 20 mg of granules is probably below the limit of detection of this method.

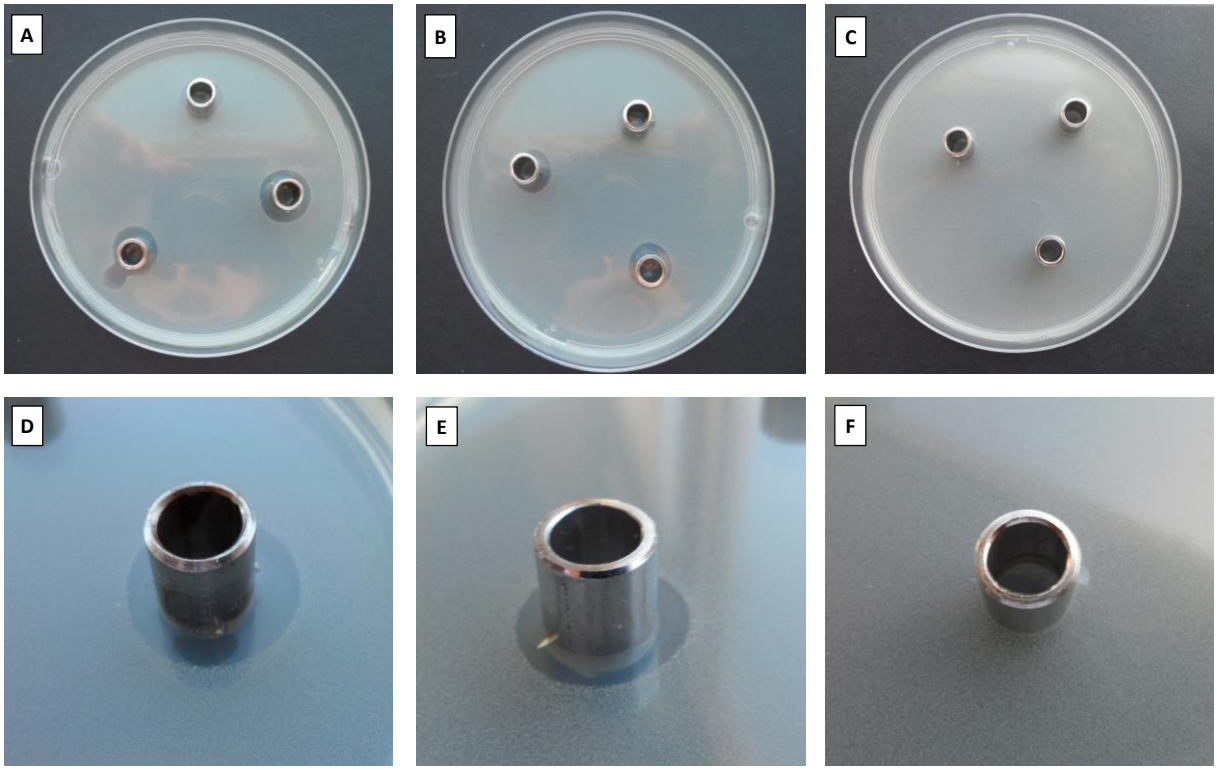


**Figure 20:** Vancomycin bioactivity assessed with diffusion method for three different releasing times. (A, D) 0.25 h; (B, E) 24 h; (C, F) 120 h.

As the diffusion method was not adequate to assess the bioactivity of vancomycin, another method was used to evaluate the capacity to inhibit *S. aureus* growth. It was observed that vancomycin was able to inhibit *S. aureus* growth in all 8 replicates until 216 h of release (Table 4 and Figure 22). In the presence of vancomycin, the total number of bacteria is significantly lower when compared with *S. aureus* for 0 and 24 h of incubation (Figure 22). After 216 h of release, the inhibition of bacterial growth was not detected for all replicates and after 288 h *S. aureus* grew in all replicates. This fact can be explained since the used method requires a dilution, leading to the final concentrations indicated on Table 4. After 216 h, the concentrations of vancomycin used in this assay were very close or below the *S. aureus* ATCC 25923 MIC (76).

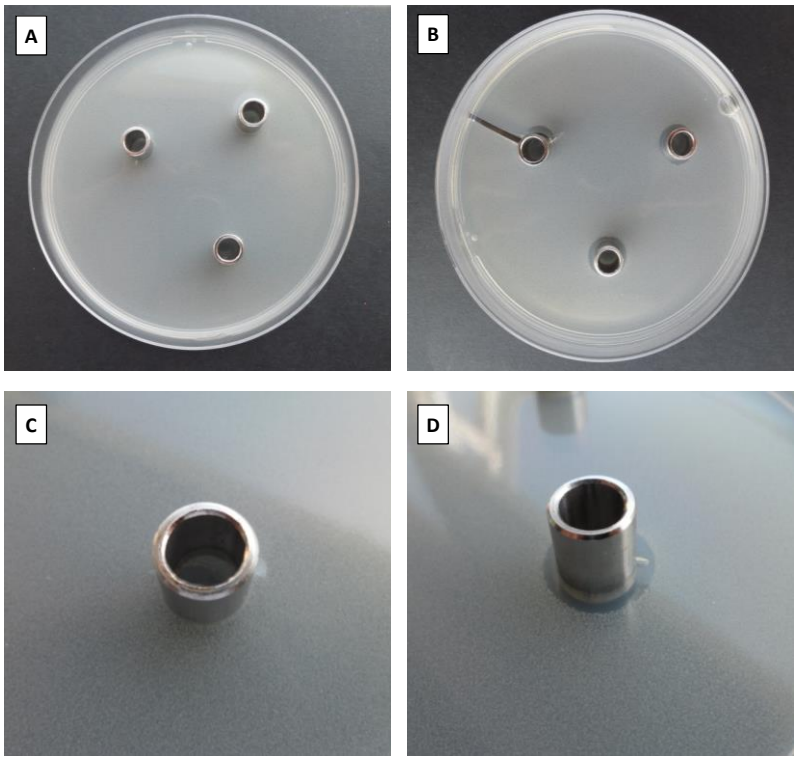


**Figure 21:** Vancomycin bioactivity studied with diffusion method for 120 h of releasing. (A, C) 20 mg of granules; (B, D) 50 mg of granules.

**Table 4:** *S. aureus* growth inhibition for each time point of released vancomycin. (-) No growth; (+) Growth in 1 replicate; (++) Growth in 2 replicates; (+++) Growth in 5 replicates.

| | time (h) | | | | | | | | | | | | | | | | |
|---|---|---|---|---|---|---|---|---|---|---|---|---|---|---|---|---|---|
| | **0.25** | **0.50** | **1.5** | **2.5** | **3.5** | **24** | **48** | **72** | **96** | **120** | **144** | **168** | **192** | **216** | **240** | **264** | **288** |
| **Vancomycin (µg/mL)** | 2.254 | 2.258 | 2.198 | 2.170 | 2.217 | 2.281 | 2.096 | 2.069 | 2.069 | 1.791 | 1.911 | 1.457 | 1.133 | 1.272 | 1.133 | 0.814 | 0.786 |
| ***S. aureus* growth** | - | - | - | - | - | - | - | - | - | - | - | - | - | - | + | ++ | +++ |

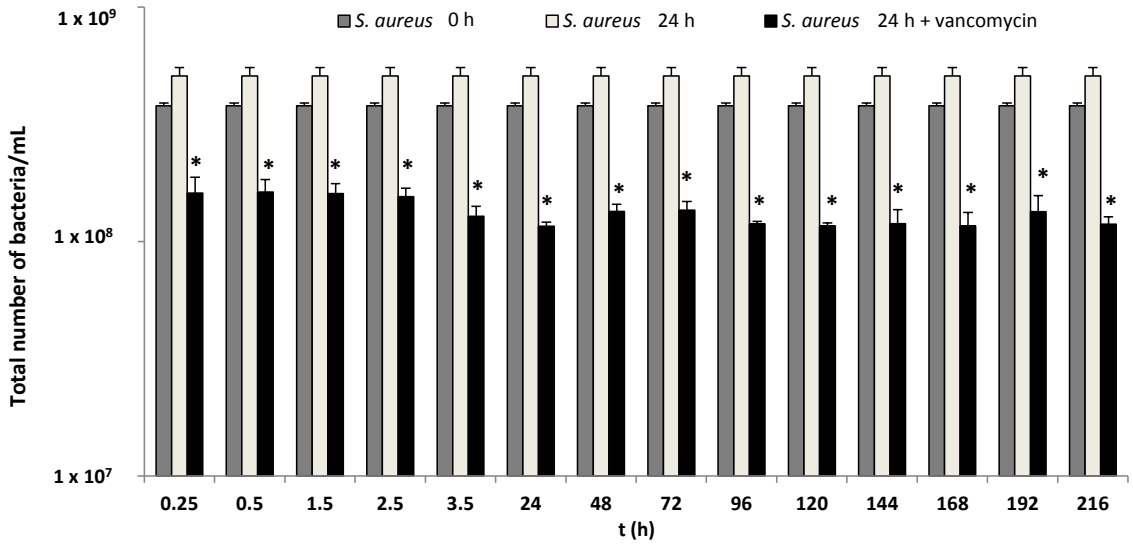


**Figure 22:** Total number of *S. aureus* in the absence of vancomycin, for 0 and 24 h of incubation, and in the presence of vancomycin after 24 h of incubation. * represents a statistical significant difference when compared with *S. aureus* 0 h and *S. aureus* 24 h ($p<0.05$).

## 3.4. *S. aureus* adhesion on granules

The results obtained indicate that *S. aureus* adhere more on granules containing collagen rather than on nanoHA granules (Figure 23). There was no difference in *S. aureus* adhesion comparing the granules containing collagen. SEM images show that for all materials, *S. aureus* has its normal spherical shape (coccus) when adhered on granules (Figure 24) (17). Moreover, bacteria adhere alone or forming an aggregate of two bacteria. Using SEM was not possible to notice a difference in number of adherent bacteria due to porosity as bacteria can go through the pores and not be exposed. In fact, it was seen that *S. aureus* many times were adherent between the nanoHA grains (Figure 24H). For nanoHA/collagen and heparinized nanoHA/collagen granules, the bacteria sometimes preferred to be adherent close to the collagen fiber-like structures (Figure 24E and G).

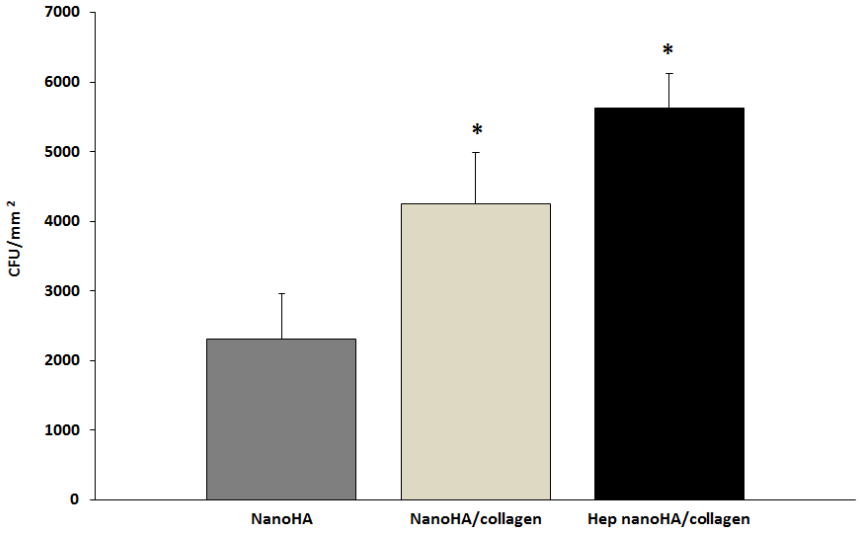


**Figure 23:** *S. aureus* adhesion on nanoHA, nanoHA/collagen and heparinized nanoHA/collagen granules expressed as CFU per $mm^2$ of granules. * represents a statistical significant difference when compared to nanoHA granules ($p<0.05$).

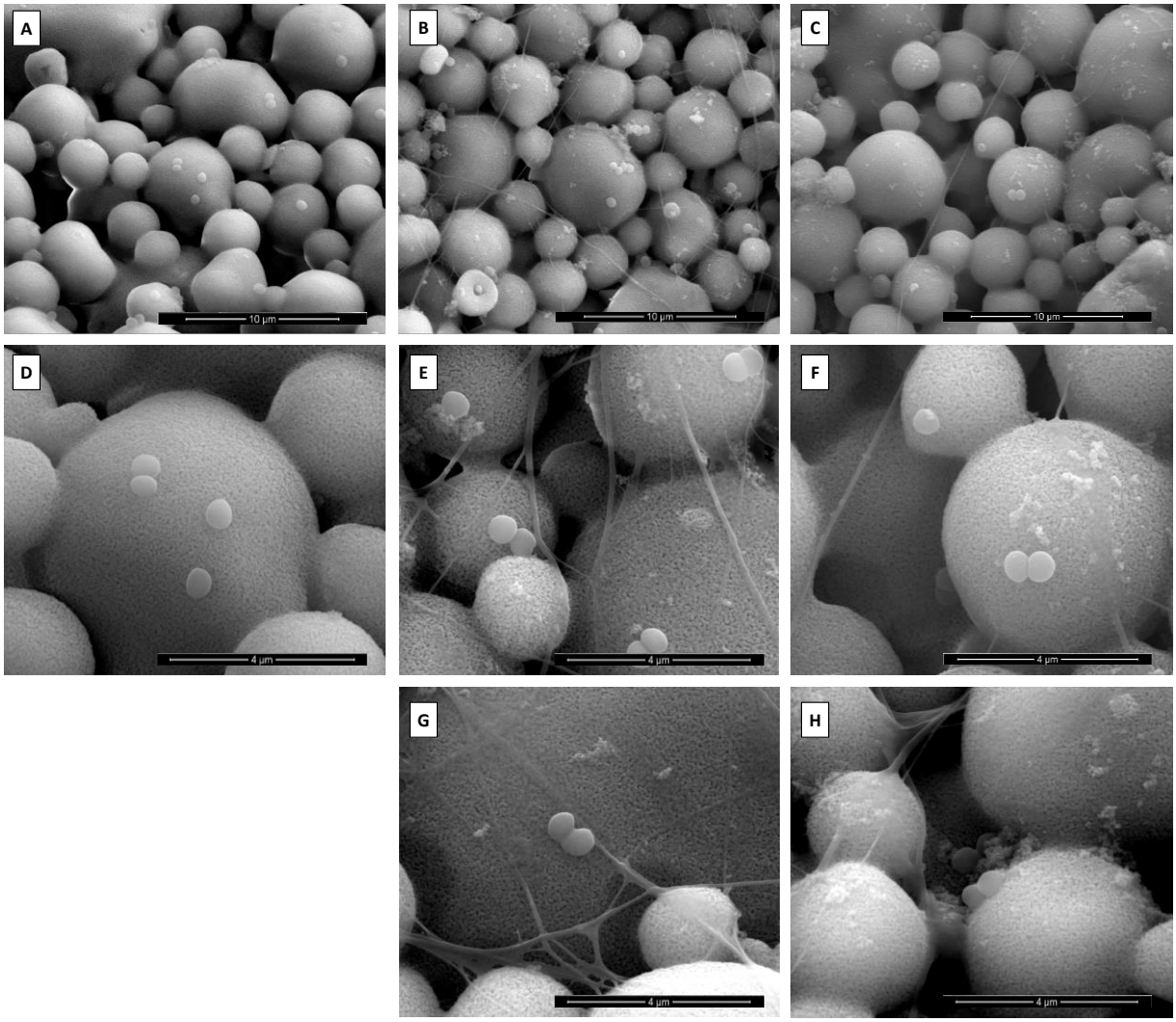


**Figure 24:** SEM images of *S. aureus* adhesion on granules. (A, D) nanoHA; (B, E, G) nanoHA/collagen; (C, F, H) heparinized nanoHA/collagen.

## 3.5. Osteoblast culture

### 3.5.1. Metabolic activity

Figure 25 indicates the results of a preliminary resazurin assay to assess the effect of vancomycin on osteoblasts metabolic activity. It was shown that vancomycin did not affect the metabolic activity of the cells for the first 24 h. However, the metabolic activity of osteoblasts in the presence of vancomycin heparinized granules decreased up to 7 days of culture. After 14 days of culture, the metabolic activity of the cells in the presence of vancomycin increases continuously until day 21 with a significant difference when compared with granules without antibiotic. Therefore, osteoblasts were able to recover when adherent on heparinized nanoHA/collagen granules.

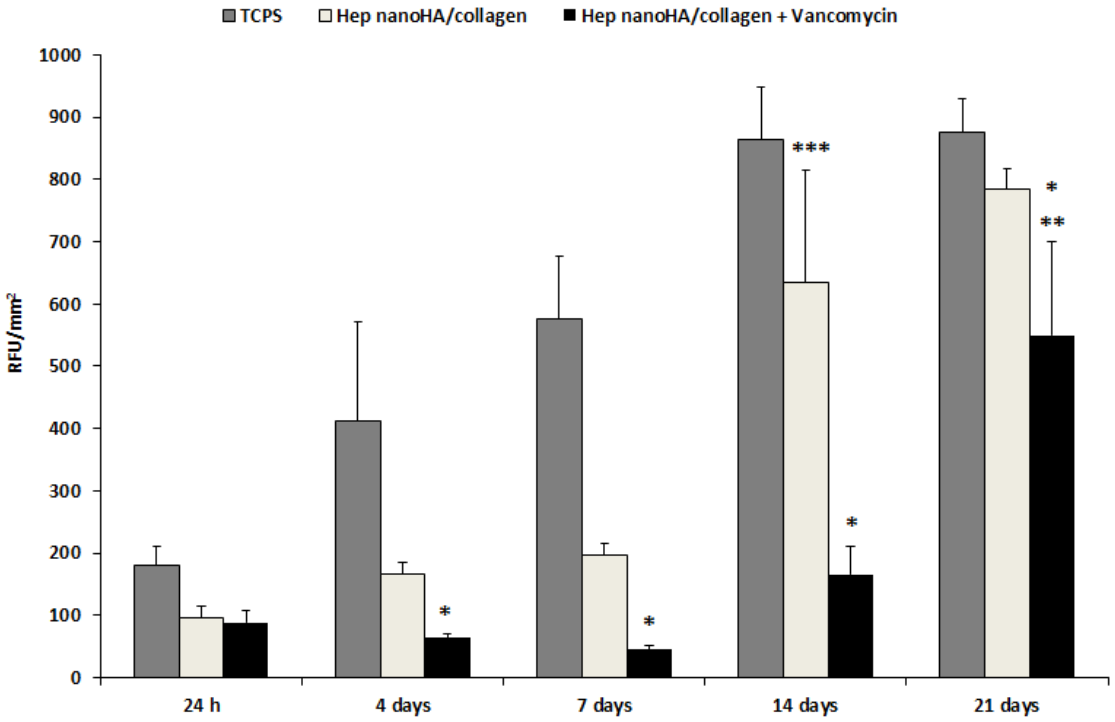


**Figure 25:** Metabolic activity of MC3T3-E1 cells cultured with heparinized nanoHA/collagen granules with and without vancomycin. Results are expressed in terms of relative fluorescence units (RFU) per $mm^2$ of granules. TCPS were used as a control. * represents a statistical significant difference when compared with heparinized nanoHA/collagen granules without vancomycin for the same time point ($p<0.05$). ** represents a statistical significant difference when compared with heparinized nanoHA/collagen granules with vancomycin at 24 h, 4, 7 and 14 days ($p<0.05$). *** represents a statistical significant difference when compared with heparinized nanoHA/collagen granules without vancomycin at 24 h, 4 and 7 days ($p<0.05$).

For heparinized nanoHA/collagen granules without vancomycin, it was observed that the metabolic activity is significantly higher at day 14, when compared with the previous time points (24 h, 4 and 7 days). Considering the heparinized nanoHA/collagen granules with vancomycin, the metabolic activity is significantly higher at day 21.

### 3.5.2. Cell Morphology

Using CLSM, it was possible to assess the MC3T3-E1 morphology on heparinized nanoHA/collagen granules, with and without vancomycin (Figure 26). At 24h of culture, less adherent cells on granules were observed for both samples. However, in the absence of antibiotic, the cells acquired a more elongated morphology even at day 1, being more evident from day 4 and maintaining that morphology until day 14. Regarding the granules with vancomycin, after 1 and 4 days of culture, the cells presented a round morphology. However, after 7 days of culture, the cells started to have a more elongated shape. After 14 days, it was evident the proliferation of cells for both samples, maintained an elongated shape and spread all over the granules surface.

The results obtained with SEM (Figure 27) were in accordance with the ones obtained by CLSM. In the absence of vancomycin, cells were able to adhere and spread on surface since the first day of culture. In opposition, for the granules containing vancomycin, cells presented a round morphology in the first 24 h. Only after 4 days of culture, cells start to exhibit an elongated shape but still with round cells present. At the end of cell culture (14 days), both samples present cell with elongated shape and spread on granules surface.

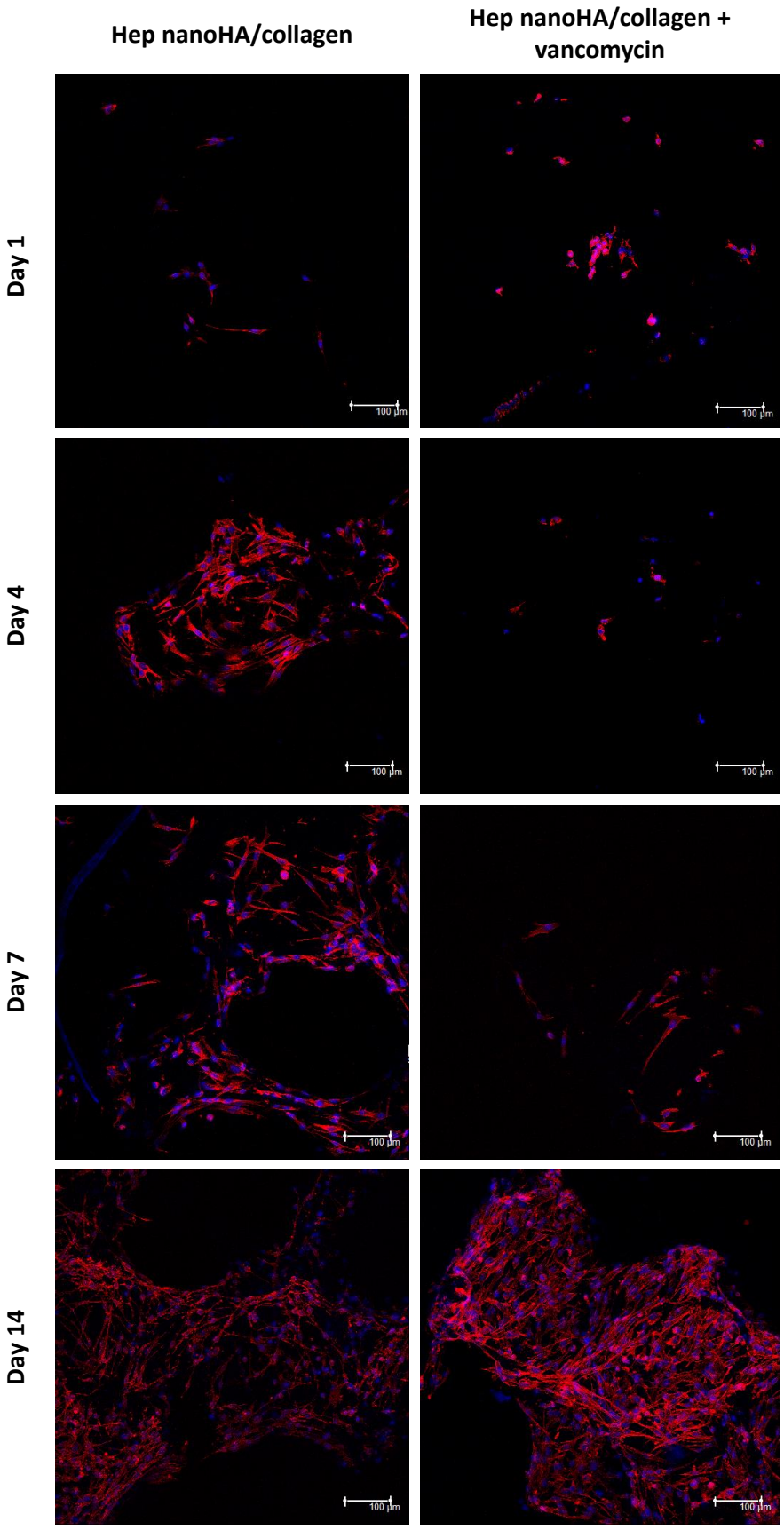


**Figure 26:** MC3T3-E1 morphology and cytoskeleton organization on heparinized nanoHA/collagen granules using CLSM after 1, 4, 7 and 14 days of culture with and without vancomycin release. F-actin is represented in red while cell nuclei were counterstained in blue with Hoechst stain. MC3T3-E1 on TCPS was used as a control (data not shown).

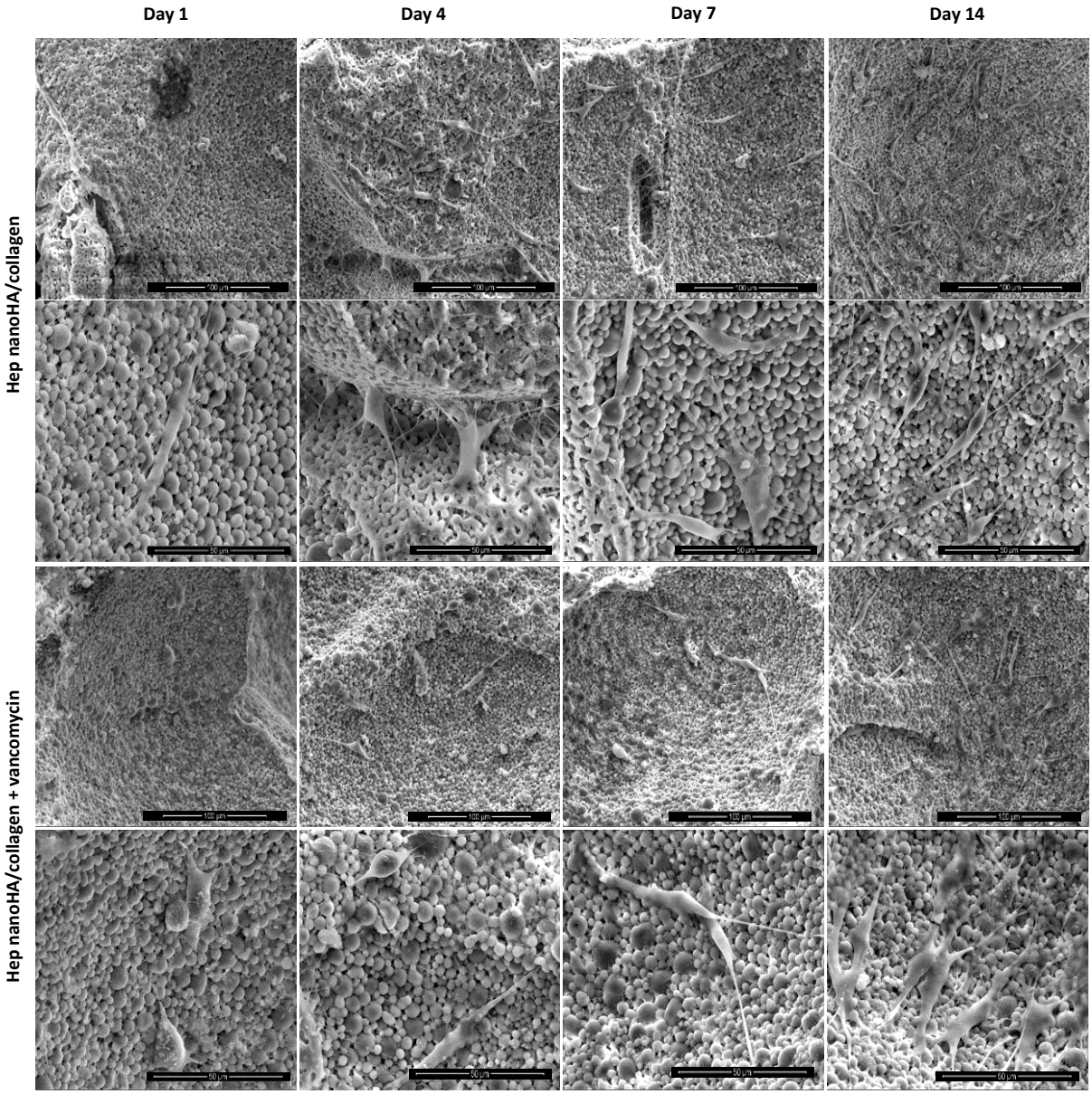


**Figure 27:** SEM images of MC3T3-E1 cells on heparinized nanoHA/collagen granules with and without vancomycin.

# Chapter 4: Discussion

The aim of this work was the production of heparinized nanoHA/collagen granules to be used as a controlled releasing system for vancomycin applied in cases of osteomyelitis. The material should be able to release the antibiotic in a sustainable way and eradicate the pathogen. Since osteomyelitis causes bone necrosis, the biocomposite should induce bone regeneration.

The first step was to produce nanoHA scaffods with macroporosity and enough resistance to be transformed into nanoHA granules. With that aim, different amounts of Dolapix CE64, a dispersive and deflocculating agent that is known to change the viscosity of the ceramic slurry and improve the impregnation method were tested (77). However, this DA can affect the porosity of the material as deflocculated suspensions may lead to higher density cast walls (78). Therefore, it was necessary to achieve a balance between adequate density and porosity. For the different volumes of Dolapix tested, it was observed that 200 µL was the most adequate, when compared with the two other volumes (150 and 250 µL). Using 200 µL, it was evident the presence of macroporosity and microporosity on nanoHA scaffolds. The resistance of the scaffold was enough to be fractured into granules and perform the following biological studies (Figure 11D, E and F). The scaffolds produced with 150 µL were too brittle and impossible to transform into granules. For the slurry containing 250 µL, the scaffolds had adequate macroporosity but the nanoHA grains presented coalescence, compromising the microporosity (Figure 11H and I).

The produced granules presented adequate dimensions (1.18-1.70 mm), strength and macroporosity to be used in cases of osteomyelitis since the defects caused by this infection normally are on the centimeters range in humans (79, 80). In addition, the size of the granules is also adequate to perform *in vivo* studies using an osteomyelitis rat model (81). Moreover, there are granules for bone substitution with similar dimensions (1-2 mm) already available in the market and clinically used with success (82).

Considering the four collagen concentrations tested, 0.05 % was considered the most suitable to be enclosed on nanoHA granules as it creates a collagen fiber-like structure without completely covering the nanoHA, as it happened with the other concentrations tested. Thus, this type of collagen incorporation allows molecules, bacteria and cells to interact with both materials as it happens in bone. Figure 14 illustrates some characteristics of the nanoHA/collagen granules. Interconnective porosity between macropores (Figure 14A) is desirable for bone tissue engineering as interconnectivity allows cell migration, neovascularization, transport of nutrients and proteins. Moreover, the presence of macroporosity induces osteoinduction (83, 84). Therefore, this 3D

structure will provide adequate environment for bone regeneration in cases of osteomyelitis, as bone tissue undergoes necrosis and requiring regeneration. Furthermore, it was evident the presence of micro (Figure 14E) and nanoporosity (Figure 14F) on nanoHA. Microporosity is known to result in higher surface area that induces protein adsorption, ion exchange and bone-like apatite formation (85). The presence of nanoporosity also improves protein adsorption and also enhances initial cell attachment (86) due to the large surface to volume ratio (48). FTIR spectra shown that the sintering process did not modify the HA composition of the nanoHA powder. Moreover, the expected amide peaks were obtained for the samples containing collagen. Using micro-CT, it was only possible to assess microporosity, as the equipment it is not sensitive enough to determine nanoporosity. Since the collagen fibers are transparent to X-rays, it was also impossible to detect collagen on granules. The average porosity of the granules is 62.7 ± 1.5 % being an adequate porosity for bone regeneration (85). The value of surface area (26.6 ± 5.6 $mm^2$) is considered high, taking into account the dimension range of these granules (1.18-1.70 mm). The average mean pore size obtained was 227.3 ± 7.2 µm, which is adequate for osteogenesis. The minimum requirement for pore size is approximately 100 µm due to cell size and cell migration (85). Particularly, the produced granules have adequate porosity for osteoblasts since the average size of an osteoblast is 20-30 µm (87).

Considering the vancomycin release from granules, it was seen that heparinized nanoHA/collagen granules are able to release higher amounts of antibiotic in a more sustainable way, when compared with nanoHA and nanoHA/collagen granules. The released vancomycin concentrations were always above *S. aureus* MIC and below MTC (37). Therefore, the released vancomycin is enough to inhibit *S. aureus* growth without being toxic. Comparing the nanoHA with nanoHA/collagen granules, similar vancomycin releasing profile was observed. Vancomycin could be adsorbed on nanoHA, since HA was already been reported as a drug carrier for vancomycin (20, 21, 56, 88). As mentioned before, vancomycin is a glycopeptide and also a cationic molecule at acidic and physiological pH, the adsorption and releasing conditions, respectively. That interaction between HA and vancomycin can be explained because HA is mostly negative (89), so cationic vancomycin can adsorb on HA. In addition, it was expected that the presence of collagen on granules would somehow cause a more controlled release, when compared to nanoHA alone, since the combination with a polymer had been reported to slow down the releasing profile (90), but that behavior was not observed. Probably because collagen is positively charged during vancomcyin adsorption (acidic pH) (91) being unlikely that these two molecules interact strongly as they both have the same charge (92). Therefore, the similar releasing profile of these two type of granules probably is dependent on HA and the presence of nanoporosity. As both granules have this type of porosity, vancomycin molecules can be more entrapped on the structure and consequently released slowlier (43). The difference observed for

heparinized nanoHA/collagen granules can be explained as heparin contains negatively charged groups (carboxylic and sulfur) and demonstrates a tendency for protein binding (93). Consequently, vancomycin has two characteristics that promote its interaction with heparin as it is a cation and a glycopeptide, increasing its adsorption. The release of vancomycin from granules can be explained for a change in the net charge of this antibiotic, as granules were placed in a solution at physiological pH (PBS solution) and vancomycin net charge decreased, becoming less positive (33, 34). Therefore, the interaction between vancomycin and the granules became weaker and vancomycin was released. However, it is important to keep in mind that in cases of infection, the environment usually has an acidic pH (94). Therefore, the releasing profile may be different.

Regarding the released vancomycin bioactivity, it was proved that the diffusion method is not ideal to determine the vancomycin bioactivity. Using broth microdilution method, it was shown that the released antibiotic was able to inhibit *S. aureus* growth in all replicates until the releasing time of 216 h. Figure 22 illustrates that in the presence of vancomycin, the total number of bacteria was lower, when compared with *S. aureus* for 0 and 24 h of incubation. Therefore, in the presence of antibiotic, the total number of bacteria was lower than the number of bacteria present in the beginning of this assay. In addition, it was also observed that in the bacteria were able to grow after 24 h of incubation in the absence of vancomycin. After 216 h of release, vancomycin was not capable to inhibit *S. aureus* growth in all replicates but this was related to the concentration used on the chosen method. The latter requires a 10 fold dilution of released vancomycin concentration, therefore decreasing the actual values to figures close or below MIC (Table 4), and leading to inhibition failure. However, it is important to retain that the released concentrations were always above vancomycin MIC for *S. aureus* ATCC 25923 (76) (Figure 18) and, if not diluted, would be able to inhibit bacterial growth.

Considering the adhesion studies of *S. aureus* on granules, a higher adhesion on granules containing collagen was detected, when compared to nanoHA granules (Figure 23). The adherence of *S. aureus* to nanoHA has already been reported, so it was expected the adherence of bacteria to this material (95, 96). A higher adherence of *S. aureus* on granules containing collagen when compared with nanoHA was also expected, since collagen is one of the ECM proteins where *S. aureus* binds to colonialize the host tissues (97, 98). Considering the heparinized nanoHA granules, it was also expect that *S. aureus* adhere more onto this material than on nanoHA as heparin is a glycosaminoglycan to which these bacteria can adhere in animals (62, 99). The higher adherence of *S. aureus* on granules may improve its eradication since the bacteria will have tendency to migrate towards the material.

As heparinized nanoHA/collagen granules proved to be the best material for vancomycin release, the effect of this antibiotic on osteoblasts metabolic activity was studied. Therefore, a preliminary MC3T3-E1 culture experiment was performed, showing that vancomycin did not affect the cells

metabolic activity during the first 24 h (Figure 25). However, the metabolic activity decreased until day 7, compared with the heparinized nanoHA/collagen granules without antibiotic. From CLSM and SEM studies, a reduced number of cells at day 1, 4 and 7 was also detected for the samples containing vancomcyin. The low metabolic activity and cell number matches with the period during which higher amounts of vancomycin were released from granules. Nevertheless, this result was not expected since vancomycin is considered a relatively safe antibiotic for osteoblasts, as a concentration of 2000 μg/mL only reduced the cell number in less than 25 % in a study performed by Rathbone *et al.* (36). However, those authors also mention that even if the antibiotic presents some toxicity, is important to consider if surviving cells remain viable and have osteogenic potential. It was observed that after 21 days of culture, the metabolic activity of MC3T3-E1 cells on granules containing vancomycin significantly increased, when compared to shorter time points. That indicates that the remaining viable cells were able to recover and proliferate, as it is observed with CLSM (Figure 26) and SEM images (Figure 27). In fact, osteoblasts in the presence of vancomycin start to increase their metabolic activity and proliferate at day 14, which is the period when vancomycin releasing ended. Therefore, after vancomycin releasing, the osteoblasts that remained viable begun to recover from the presence of antibiotic. The obtained results for this preliminary assay are promising since osteoblasts were able to adhere and proliferate even in the presence of vancomycin.

# Chapter 5: Concluding remarks and future work

## 5.1. Concluding remarks

In this study, heparinized nanoHA/collagen granules were successfully produced. These granules have porosity ranging from macro to nano, which are important characteristics for cell adhesion, migration and protein adsorption. In addition, these granules have a collagen fiber-like structure with appropriate distribution, enabling both materials to be available to interact with bone environment. Moreover, these granules are adequate to be used in cases of osteomyelitis since they have adequate size for *in vivo* experiments and clinical assays.

When compared to nanoHA and nanoHA/collagen granules, the heparinized nanoHA/collagen granules were able to release higher amounts of vancomycin in a more sustainable way during 360 h. Furthermore, the released concentration was always above *S. aureus* MIC and below MTC. Therefore, the released vancomycin was able to inhibit bacterial growth and possibly without any toxicity for the organism. In fact, it was proved that the released antibiotic was bioactive and inhibited *S. aureus* growth for at least 216 h.

Regarding *S. aureus* adhesion, it was observed that bacteria adhere more on granules containing collagen. This probably results from the fact that collagen is one ECM protein where *S. aureus* adhere to colonialize the host tissue. This characteristic may induce the bacteria to migrate onto the material and be in contact with the antibiotic, improving the therapeutic effect.

Preliminary results obtained for osteoblasts cell culture shown that the released vancomycin negatively affects the metabolic activity between 4 and 7 days of culture. Those time points match with higher values of vancomycin concentration. However, the metabolic activity increases between 14 days and 21 days, when the release of vancomycin almost or has already ceased. Therefore, the cells that remained viable were able to recover and proliferate. In fact, SEM and CLSM images illustrated the osteoblasts covering the granules surface.

As a conclusion, the produced heparinized nanoHA/collagen granules are a promising and innovative material to be used in the treatment of osteomyelitis. Grafting this biocomposite with heparin enables a sustainable release of vancomycin, in concentrations capable to inhibit *S. aureus* growth and without being toxic. Moreover, osteoblasts are capable to adhere on the surface of granules containing antibiotic. The cells that remained viable were able to proliferate and covered the entire surface after 14 days of culture. In that sense, the aim of the work was fully attended since bacterial

growth was inhibited, osteoblasts were able to proliferate and bone regeneration probably will be possible.

## 5.2. Future work

Considering the results obtained in this work, there are some aspects that need to be improved and some new ideas must be explored, so that the performance of this drug releasing and tissue regeneration-inducing material might be enhanced. One important thing to evaluate is the releasing profile of vancomycin from heparinized nanoHA/collagen granules on human serum and infection environment, to better mimic the osteomyelitis scenario.

As *S. aureus* is not the only pathogen involved in osteomyelitis, it would be important to study the bioactivity of vancomycin with other bacteria such as *Staphylococcus epidermidis* as well as MRSA, since these two bacteria are frequent pathogens identified in patients with osteomyelitis. An additional possibility is to study the bioactivity of vancomycin on VRSA, as the appearance of vancomycin resistant strains is becoming more frequent.

Regarding the cell culture with MC3T3-E1, it is necessary to repeat this assay to validate the preliminary results obtained. In addition, it would be important to perform tests to evaluate the biochemical markers expressed by these cells, in order to confirm the presence of the typical osteoblasts phenotype and corresponding behavior. Moreover, a co-culture system containing osteoblasts and osteoclasts would be interesting to determine the influence of the material and the antibiotic on an environment comprehending the two cell types, as it would better mimic bone tissue.

Moreover, the performance of *in vivo* studies on osteomyelitis rat models is crucial to assess the possible effectiveness of this material in the treatment of this infection.

# References


1. Meyer HS. Color Textbook of Histology. 3 ed: Saunders; 2001.
2. Salgado AJ, Coutinho OP, Reis RL. Bone Tissue Engineering: State of the Art and Future Trends. Macromolecular Bioscience. 2004;4(8):743-65.
3. Cohen Jr MM. The new bone biology: Pathologic, molecular, and clinical correlates. American Journal of Medical Genetics Part A. 2006;140A(23):2646-706.
4. Meinel L, Fajardo R, Hofmann S, Langer R, Chen J, Snyder B, et al. Silk implants for the healing of critical size bone defects. Bone. 2005;37(5):688-98.
5. Gartner LP, Hiatt JL, Strum JM. Cell biology and histology. 6 ed: Wolters Kluwer Health/Lippincott Williams & Wilkins; 2011.
6. Taton TA. Nanotechnology. Boning up on biology. Nature. 2001;412(6846):491-2.
7. Cowin SC, Hegedus DH. Bone remodeling I: theory of adaptive elasticity. Journal of Elasticity. 1976;6(3):313-26.
8. Raisz LG. Physiology and Pathophysiology of Bone Remodeling. Clinical Chemistry. 1999;45(8):1353-8.
9. Baskot B. Coronary Angiography - Advances in Noninvasive Imaging Approach for Evaluation of Coronary Artery Disease. 1 ed: InTech; 2011.
10. Lew DP, Waldvogel FA. Osteomyelitis. The Lancet. 2004;364(9431):369-79.
11. Carek PJ, Dickerson LM, Sack JL. Diagnosis and management of osteomyelitis. 2001;63(12):2413-21.
12. Brady RA, Leid JG, Calhoun JH, Costerton JW, Shirtliff ME. Osteomyelitis and the role of biofilms in chronic infection. FEMS Immunology & Medical Microbiology. 2008;52(1):13-22.
13. Hatzenbuehler J, Pulling T. Diagnosis and management of osteomyelitis. American family physician. 2011;84(9):1027-33.
14. Naimi TS, LeDell KH, Como-Sabetti K, Borchardt SM, Boxrud DJ, Etienne J, et al. Comparison of Community- and Health Care–Associated Methicillin-Resistant *Staphylococcus aureus* Infection. JAMA: The Journal of the American Medical Association. 2003;290(22):2976-84.
15. Harris LG, Richards RG. Staphylococci and implant surfaces: a review. Injury. 2006;37(2):S3-S14.
16. Tiemersma EW, Bronzwaer SLAM, Lyytikäinen O, Degener JE, Schrijnemakers P, Bruinsma N, et al. Methicillin-resistant *Staphylococcus aureus* in Europe, 1999-2002. Emerging Infectious Diseases. 2004;10(9):1627-34.
17. Willey JM, Sherwood L, Woolverton CJ. Prescott, Harley, and Klein's Microbiology. 7 ed: McGraw-Hill Higher Education; 2008.
18. Gordon RJ, Lowy FD. Pathogenesis of Methicillin-Resistant *Staphylococcus aureus* Infection. Clinical Infectious Diseases. 2008;46:S350-S9.
19. Landersdorfer CB, Kinzig M, Bulitta JB, Hennig FF, Holzgrabe U, Sörgel F, et al. Bone Penetration of Amoxicillin and Clavulanic Acid Evaluated by Population Pharmacokinetics and Monte Carlo Simulation. Antimicrobial Agents and Chemotherapy. 2009;53(6):2569-78.
20. Jiang JL, Li YF, Fang TL, Zhou J, Li XL, Wang YC, et al. Vancomycin-loaded nano-hydroxyapatite pellets to treat MRSA-induced chronic osteomyelitis with bone defect in rabbits. Inflammation research. 2012;61(3):207-15.
21. Ravelingien M, Mullens S, Luyten J, D'Hondt M, Boonen J, De Spiegeleer B, et al. Vancomycin release from poly(D,L-lactic acid) spray-coated hydroxyapatite fibers. European journal of pharmaceutics and biopharmaceutics. 2010;76(3):366-70.
22. Jacqueline C, Amador G, Caillon J, Le Mabecque V, Batard E, Miègeville A-F, et al. Efficacy of the new cephalosporin ceftaroline in the treatment of experimental methicillin-resistant *Staphylococcus aureus* acute osteomyelitis. Journal of Antimicrobial Chemotherapy. 2010;65(8):1749-52.

23. Buszewski B, Szultka M, Olszowy P, Bocian S, Ligor T. A novel approach to the rapid determination of amoxicillin in human plasma by solid phase microextraction and liquid chromatography. Analyst. 2011;136(12):2635-42.
24. Martins VCA, Goissis G, Ribeiro AC, Marcantônio Jr E, Bet MR. The Controlled Release of Antibiotic by Hydroxyapatite: Anionic Collagen Composites. Artificial Organs. 1998;22(3):215-21.
25. Rybak MJ. The Pharmacokinetic and Pharmacodynamic Properties of Vancomycin. Clinical Infectious Diseases. 2006;42(1):S35-S9.
26. Schäfer M, Schneider TR, Sheldrick GM. Crystal structure of vancomycin. Structure. 1996;4(12):1509-15.
27. Williams DH, Bardsley B. The Vancomycin Group of Antibiotics and the Fight against Resistant Bacteria. Angewandte Chemie International Edition. 1999;38(9):1172-93.
28. Sattur A, Lee J-H, Song K-B, Panda T, Kim C-H, Rhee S-K, et al. Analytical techniques for vancomycin—A review. Biotechnol Bioprocess Eng. 2000;5(3):153-8.
29. Levine DP. Vancomycin: A History. Clinical Infectious Diseases. 2006;42(1):S5-S12.
30. Hasper HE, Kramer NE, Smith JL, Hillman JD, Zachariah C, Kuipers OP, et al. An Alternative Bactericidal Mechanism of Action for Lantibiotic Peptides That Target Lipid II. Science. 2006;313(5793):1636-7.
31. Hadaway L, Chamallas SN. Vancomycin: new perspectives on an old drug. Journal of Infusion Nursing. 2003;26(5):278-84.
32. Lai C-Y, Trewyn BG, Jeftinija DM, Jeftinija K, Xu S, Jeftinija S, et al. A mesoporous silica nanosphere-based carrier system with chemically removable CdS nanoparticle caps for stimuli-responsive controlled release of neurotransmitters and drug molecules. Journal of the American Chemical Society. 2003;125(15):4451-9.
33. Vijan LE. The interaction of vancomycin with DNA. Rev Roum Chem. 2009;54(10):807-13.
34. Johnson JL, Yalkowsky SH. Reformulation of a new vancomycin analog: an example of the importance of buffer species and strength. AAPS PharmSciTech. 2006;7(1):E33-E7.
35. Slowing II, Vivero-Escoto JL, Wu C-W, Lin VSY. Mesoporous silica nanoparticles as controlled release drug delivery and gene transfection carriers. Advanced Drug Delivery Reviews. 2008;60(11):1278-88.
36. Rathbone CR, Cross JD, Brown KV, Murray CK, Wenke JC. Effect of various concentrations of antibiotics on osteogenic cell viability and activity. Journal of Orthopaedic Research. 2011;29(7):1070-4.
37. Dion A, Langman M, Hall G, Filiaggi M. Vancomycin release behaviour from amorphous calcium polyphosphate matrices intended for osteomyelitis treatment. Biomaterials. 2005;26(35):7276-85.
38. Andrews JM. Determination of minimum inhibitory concentrations. Journal of Antimicrobial Chemotherapy. 2001;48(1):5-16.
39. Rybak MJ, Hershberger E, Moldovan T, Grucz RG. In Vitro Activities of Daptomycin, Vancomycin, Linezolid, and Quinupristin-Dalfopristin against Staphylococci and Enterococci, Including Vancomycin- Intermediate and -Resistant Strains. Antimicrobial Agents and Chemotherapy. 2000;44(4):1062-6.
40. Lamp K, Rybak M, Bailey E, Kaatz G. *In vitro* pharmacodynamic effects of concentration, pH, and growth phase on serum bactericidal activities of daptomycin and vancomycin. Antimicrobial agents and chemotherapy. 1992;36(12):2709-14.
41. Chang S, Sievert DM, Hageman JC, Boulton ML, Tenover FC, Downes FP, et al. Infection with Vancomycin-Resistant *Staphylococcus aureus* Containing the vanA Resistance Gene. New England Journal of Medicine. 2003;348(14):1342-7.
42. Fei J, Liu G-d, Pan C-j, Chen J-y, Zhou Y-g, Xiao S-h, et al. Preparation, release profiles and antibacterial properties of vancomycin-loaded Ca–P coating titanium alloy plate. Journal of Materials Science: Materials in Medicine. 2011;22(4):989-95.

43. Ginebra MP, Traykova T, Planell JA. Calcium phosphate cements as bone drug delivery systems: a review. Journal of controlled release : official journal of the Controlled Release Society. 2006;113(2):102-10.
44. Kalita SJ, Bhardwaj A, Bhatt HA. Nanocrystalline calcium phosphate ceramics in biomedical engineering. Materials Science and Engineering: C. 2007;27(3):441-9.
45. Mostafa NY, Brown PW. Computer simulation of stoichiometric hydroxyapatite: Structure and substitutions. Journal of Physics and Chemistry of Solids. 2007;68(3):431-7.
46. Teixeira S, Rodriguez MA, Pena P, De Aza AH, De Aza S, Ferraz MP, et al. Physical characterization of hydroxyapatite porous scaffolds for tissue engineering. Materials Science and Engineering: C. 2009;29(5):1510-4.
47. Guo L, Huang M, Zhang X. Effects of sintering temperature on structure of hydroxyapatite studied with Rietveld method. Journal of Materials Science: Materials in Medicine. 2003;14(9):817-22.
48. Laranjeira MS, Fernandes MH, Monteiro FJ. Innovative macroporous granules of nanostructured-hydroxyapatite agglomerates: Bioactivity and osteoblast-like cell behaviour. Journal of Biomedical Materials Research Part A. 2010;95A(3):891-900.
49. Riman RE, Suchanek WL, Byrappa K, Chen C-W, Shuk P, Oakes CS. Solution synthesis of hydroxyapatite designer particulates. Solid State Ionics. 2002;151(1–4):393-402.
50. Ahn ES, Gleason NJ, Nakahira A, Ying JY. Nanostructure Processing of Hydroxyapatite-based Bioceramics. Nano Letters. 2001;1(3):149-53.
51. Werner J, Linner-Krčmar B, Friess W, Greil P. Mechanical properties and in vitro cell compatibility of hydroxyapatite ceramics with graded pore structure. Biomaterials. 2002;23(21):4285-94.
52. DA Wahl JC. Collagen-hydroxyapatite composites for hard tissue repair. European Cells and Materials. 2006;11:43-56.
53. Ferraz MP, Monteiro FJ, Manuel CM. Hydroxyapatite nanoparticles: A review of preparation methodologies. Journal of Applied Biomaterials & Biomechanics. 2004;2(2):74-80.
54. Ribeiro N, Sousa SR, Monteiro FJ. Influence of crystallite size of nanophased hydroxyapatite on fibronectin and osteonectin adsorption and on MC3T3-E1 osteoblast adhesion and morphology. Journal of Colloid and Interface Science. 2010;351(2):398-406.
55. Wei G, Ma PX. Structure and properties of nano-hydroxyapatite/polymer composite scaffolds for bone tissue engineering. Biomaterials. 2004;25(19):4749-57.
56. Rauschmann MA, Wichelhaus TA, Stirnal V, Dingeldein E, Zichner L, Schnettler R, et al. Nanocrystalline hydroxyapatite and calcium sulphate as biodegradable composite carrier material for local delivery of antibiotics in bone infections. Biomaterials. 2005;26(15):2677-84.
57. Rossert J, Eberspaecher H, de Crombrugghe B. Separate cis-acting DNA elements of the mouse pro-alpha 1(I) collagen promoter direct expression of reporter genes to different type I collagen-producing cells in transgenic mice. The Journal of Cell Biology. 1995;129(5):1421-32.
58. Lee CH, Singla A, Lee Y. Biomedical applications of collagen. International Journal of Pharmaceutics. 2001;221(1–2):1-22.
59. Cen L, Liu W, Cui L, Zhang W, Cao Y. Collagen tissue engineering: development of novel biomaterials and applications. Pediatric research. 2008;63(5):492-6.
60. Buehler MJ, Keten S, Ackbarow T. Theoretical and computational hierarchical nanomechanics of protein materials: Deformation and fracture. Progress in Materials Science. 2008;53(8):1101-241.
61. Kikuchi M, Itoh S, Ichinose S, Shinomiya K, Tanaka J. Self-organization mechanism in a bone-like hydroxyapatite/collagen nanocomposite synthesized *in vitro* and its biological reaction *in vivo*. Biomaterials. 2001;22(13):1705-11.
62. Ljungh Å, Moran AP, Wadström T. Interactions of bacterial adhesins with extracellular matrix and plasma proteins: pathogenic implications and therapeutic possibilities. FEMS Immunology & Medical Microbiology. 1996;16(2):117-26.

63. Wissink MJB, Beernink R, Pieper JS, Poot AA, Engbers GHM, Beugeling T, et al. Immobilization of heparin to EDC/NHS-crosslinked collagen. Characterization and *in vitro* evaluation. Biomaterials. 2001;22(2):151-63.
64. Hirsh J, Raschke R. Heparin and Low-Molecular-Weight Heparin CHEST Journal. 2004;126(3):188S-203S.
65. Teixeira S, Yang L, Dijkstra P, Ferraz M, Monteiro F. Heparinized hydroxyapatite/collagen three-dimensional scaffolds for tissue engineering. Journal of Materials Science: Materials in Medicine. 2010;21(8):2385-92.
66. Conrad HE. Heparin-Binding Proteins. 1 ed: Elsevier Science; 1997.
67. Vercaigne LM, Sitar DS, Penner SB, Bernstein K, Wang GQ, Burczynski FJ. Antibiotic-Heparin Lock: *In Vitro* Antibiotic Stability Combined with Heparin in a Central Venous Catheter. Pharmacotherapy: The Journal of Human Pharmacology and Drug Therapy. 2000;20(4):394-9.
68. Droste JC, Jeraj HA, MacDonald A, Farrington K. Stability and in vitro efficacy of antibiotic–heparin lock solutions potentially useful for treatment of central venous catheter-related sepsis. Journal of Antimicrobial Chemotherapy. 2003;51(4):849-55.
69. Garland JS, Alex CP, Henrickson KJ, McAuliffe TL, Maki DG. A Vancomycin-Heparin Lock Solution for Prevention of Nosocomial Bloodstream Infection in Critically Ill Neonates With Peripherally Inserted Central Venous Catheters: A Prospective, Randomized Trial. Pediatrics. 2005;116(2):198-205.
70. Petitou M, Casu B, Lindahl U. 1976–1983, a critical period in the history of heparin: the discoveryof the antithrombin binding site. Biochimie. 2003;85(1–2):83-9.
71. Ferraz MP, Mateus AY, Sousa JC, Monteiro FJ. Nanohydroxyapatite microspheres as delivery system for antibiotics: Release kinetics, antimicrobial activity, and interaction with osteoblasts. Journal of Biomedical Materials Research Part A. 2007;81A(4):994-1004.
72. Borges A, Ferreira C, Saavedra MJ, Simões M. Antibacterial Activity and Mode of Action of Ferulic and Gallic Acids Against Pathogenic Bacteria. Microbial Drug Resistance. 2013;19(4):256-65.
73. O'Brien J, Wilson I, Orton T, Pognan F. Investigation of the Alamar Blue (resazurin) fluorescent dye for the assessment of mammalian cell cytotoxicity. European Journal of Biochemistry. 2000;267(17):5421-6.
74. Chang MC, Tanaka J. FT-IR study for hydroxyapatite/collagen nanocomposite cross-linked by glutaraldehyde. Biomaterials. 2002;23(24):4811-8.
75. Lu Q, Zhang S, Hu K, Feng Q, Cao C, Cui F. Cytocompatibility and blood compatibility of multifunctional fibroin/collagen/heparin scaffolds. Biomaterials. 2007;28(14):2306-13.
76. Bhateja P, Mathur T, Pandya M, Fatma T, Rattan A. Detection of vancomycin resistant *Staphylococcus aureus*: A comparative study of three different phenotypic screening methods. Indian Journal of Medical Microbiology. 2005;23(1):52.
77. Scalera F, Gervaso F, Sanosh KP, Sannino A, Licciulli A. Influence of the calcination temperature on morphological and mechanical properties of highly porous hydroxyapatite scaffolds. Ceramics International. 2013;39(5):4839-46.
78. Vaz L, Lopes AB, Almeida M. Porosity control of hydroxyapatite implants. Journal of Materials Science: Materials in Medicine. 1999;10(4):239-42.
79. Gitelis S, Brebach GT. The treatment of chronic osteomyelitis with a biodegradable antibiotic-impregnated implant. Journal of orthopaedic surgery. 2002;10(1):53-60.
80. Patzakis MJ, Mazur K, Wilkins J, Sherman R, Holtom P. Septopal beads and autogenous bone grafting for bone defects in patients with chronic osteomyelitis. Clinical orthopaedics and related research. 1993;295:112-8.
81. Itokazu M, Yamamoto K, Yang WY, Aoki T, Kato N, Watanabe K. The sustained release of antibiotic from freeze-dried fibrin-antibiotic compound and efficacies in a rat model of osteomyelitis. Infection. 1997;25(6):359-63.
82. Jafarian M, Eslaminejad MB, Khojasteh A, Mashhadi Abbas F, Dehghan MM, Hassanizadeh R, et al. Marrow-derived mesenchymal stem cells-directed bone regeneration in the dog mandible: a

comparison between biphasic calcium phosphate and natural bone mineral. Oral Surgery, Oral Medicine, Oral Pathology, Oral Radiology, and Endodontology. 2008;105(5):14-24.
83. Teixeira S, Oliveira S, Ferraz M, Monteiro F. Three dimensional macroporous calcium phosphate scaffolds for bone tissue engineering. Key Engineering Materials. 2008;361:947-50.
84. Rose FR, Cyster LA, Grant DM, Scotchford CA, Howdle SM, Shakesheff KM. In vitro assessment of cell penetration into porous hydroxyapatite scaffolds with a central aligned channel. Biomaterials. 2004;25(24):5507-14.
85. Karageorgiou V, Kaplan D. Porosity of 3D biomaterial scaffolds and osteogenesis. Biomaterials. 2005;26(27):5474-91.
86. Leong MF, Chian KS, Mhaisalkar PS, Ong WF, Ratner BD. Effect of electrospun poly(D,L-lactide) fibrous scaffold with nanoporous surface on attachment of porcine esophageal epithelial cells and protein adsorption. Journal of Biomedical Materials Research Part A. 2009;89A(4):1040-8.
87. Puckett S, Pareta R, Webster TJ. Nano rough micron patterned titanium for directing osteoblast morphology and adhesion. International journal of nanomedicine. 2008;3(2):229.
88. Saito T, Takeuchi R, Hirakawa K, Nagata N, Yoshida T, Koshino T, et al. Slow-releasing potential of vancomycin-loaded porous hydroxyapatite blocks implanted into MRSA osteomyelitis. Journal of Biomedical Materials Research. 2002;63(3):245-51.
89. Kojima C, Watanabe K. Adsorption and Desorption of Bioactive Proteins on Hydroxyapatite for Protein Delivery Systems. Journal of Drug Delivery. 2012;2012:1-4.
90. Kim H-W, Knowles JC, Kim H-E. Hydroxyapatite porous scaffold engineered with biological polymer hybrid coating for antibiotic Vancomycin release. Journal of Materials Science: Materials in Medicine. 2005;16(3):189-95.
91. Uquillas JA, Akkus O. Modeling the Electromobility of Type-I Collagen Molecules in the Electrochemical Fabrication of Dense and Aligned Tissue Constructs. Annals of biomedical engineering. 2012;40(8):1641-53.
92. Patil S, Sandberg A, Heckert E, Self W, Seal S. Protein adsorption and cellular uptake of cerium oxide nanoparticles as a function of zeta potential. Biomaterials. 2007;28(31):4600-7.
93. Fallgren C, Andersson A, Ljungh A. The role of glycosaminoglycan binding of staphylococci in attachment to eukaryotic host cells. Current Microbiology. 2001;43(1):57-63.
94. Fang RC, Galiano RD. Adjunctive therapies in the treatment of osteomyelitis. Seminars in plastic surgery. 2009;23(2):141.
95. Ribeiro M, Monteiro FJ, Ferraz MP. *Staphylococcus aureus* and *Staphylococcus epidermidis* adhesion to nanohydroxyapatite in the presence of model proteins. Biomedical Materials. 2012;7(4):045010.
96. Grenho L, Manso MC, Monteiro FJ, Ferraz MP. Adhesion of *Staphylococcus aureus*, *Staphylococcus epidermidis*, and *Pseudomonas aeruginosa* onto nanohydroxyapatite as a bone regeneration material. Journal of Biomedical Materials Research Part A. 2012;100A(7):1823-30.
97. Götz F. *Staphylococcus* and biofilms. Molecular Microbiology. 2002;43(6):1367-78.
98. Lew DP, Waldvogel FA. Osteomyelitis. New England Journal of Medicine. 1997;336(14):999-1007.
99. Pascu C, Ljungh Å, Wadström T. Staphylococci Bind Heparin-Binding Host Growth Factors. Current Microbiology. 1996;32(4):201-7.